Journal Pre-proofs

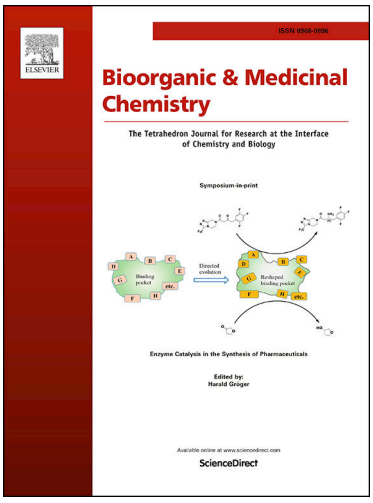

Design, synthesis and biological evaluation of anthranilamide derivatives as potent SMO inhibitors

Dezhong Ji, Wanwan Zhang, Yungen Xu, Jing-Jing Zhang

PII: S0968-0896(20)30145-0
DOI: https://doi.org/10.1016/j.bmc.2020.115354
Reference: BMC 115354

To appear in: *Bioorganic & Medicinal Chemistry*

Received Date: 9 December 2019
Revised Date: 17 January 2020
Accepted Date: 31 January 2020

Please cite this article as: D. Ji, W. Zhang, Y. Xu, J-J. Zhang, Design, synthesis and biological evaluation of anthranilamide derivatives as potent SMO inhibitors, *Bioorganic & Medicinal Chemistry* (2020), doi: https://doi.org/10.1016/j.bmc.2020.115354

Design, synthesis and biological evaluation of anthranilamide derivatives as potent SMO inhibitors

Dezhong Ji[1,a], Wanwan Zhang[1,a], Yungen Xu[1,2,*], Jing-Jing Zhang[1,2,*]

[1]Department of Medicinal Chemistry, China Pharmaceutical University, Nanjing 210009, China

[2]Jiangsu Key Laboratory of Drug Design and Optimization, China Pharmaceutical University, Nanjing 210009, China

[a]These authors contributed equally to this work.

*Corresponding author: Jing-Jing Zhang (Email:jjzhangnj@163.com; Tel: +86-025-83271244).

Keywords: Smoothened inhibitor; Hedgehog signaling pathway; ring-opening; anthranilamide; molecular dynamics

Highlights

- SMO inhibitors with novel structural features were developed by replacing the phthalazine core in LY2940680 with anthranilamide via a ring-opening strategy.
- The anthranilamide structure could mimic the phthalazine ring in LY2940680 by forming a pseudo-ring structure resulting from the intra-molecular hydrogen bond interaction between the oxygen atom of carbonyl group and hydrogen atom of the amino group.
- The pseudo-ring structure formed by anthranilamide and the hydrogen bond interaction between its carbonyl group and R400 of SMO, as evidenced by Glide docking study, suggested that the new compounds can mimic the binding conformation of LY2940680 to SMO.
- Difference in the inhibitory activity between the new compounds and LY2940680 were studied by molecular dynamic analysis.

Graphic abstract

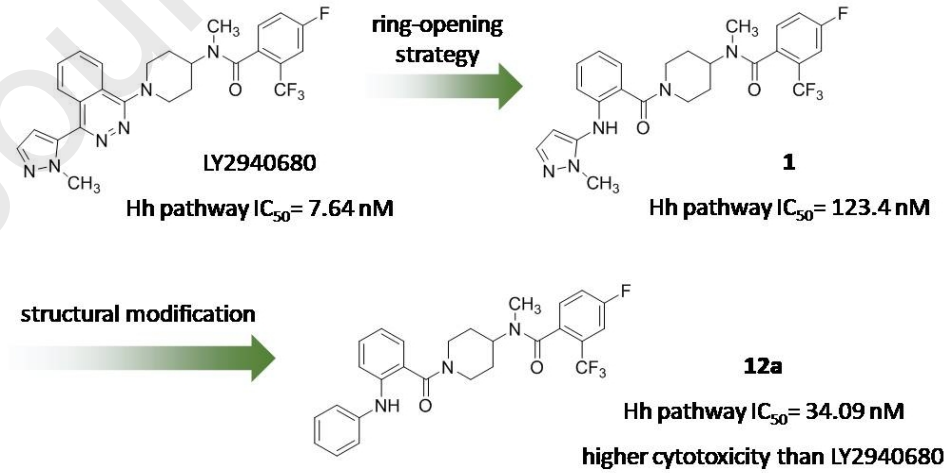

Abstract

A series of anthranilamide derivatives were designed and synthesized as novel smoothened (SMO) inhibitors based on the SMO inhibitor taladegib (LY2940680), which can also inhibit the SMO-D473H mutant, via a ring-opening strategy. The phthalazine core in LY2940680 was replaced with anthranilamide, which retained the inhibitory activity towards the hedgehog (Hh) signaling pathway as evidenced by a dual luciferase reporter gene assay. Compound**12a** displayed the best inhibitory activity against the Hh signaling pathway with IC_{50} value of 34.09nM, and exhibited better proliferation inhibitory activity towards the Daoy cell line (IC_{50}= 0.48 μM) than LY2940680 (IC_{50}= 0.79 μM).

1. Introduction

The Hedgehog (Hh) signaling pathway plays an important role in embryonic and postnatal development.[1]It involves several components including the Hh ligands, the 12-pass transmembrane receptor Patched 1 (PTCH1), the 7-pass membrane G-protein-coupled receptor smoothened (SMO), suppressor of fused (SUFU), and the zinc-finger transcription factors GLI proteins.[2] In adults, with the exception of stem cell homeostasis maintenance and tissue repair, it is mostly inactive as SMO and GLI are inhibited by PTCH1 and SUFU, respectively.[1, 3]Aberrant activation of the Hh signaling pathway is involved in the initiation and progression of various cancers, and also associated with cancer stem cell

biology.[4] Therefore, the inhibition of the Hh pathway is an attractive approach for treating cancer.[4]

The Hh pathway can be activated by the binding of the Hh ligands to PTCH1, which relives SMO from PTCH1. The activated SMO further represses SUFU, which leads to the release and nuclear translocation of the GLI proteins. These GLI proteins can promote some cancer-related gene expression.[5] Moreover, mutations of the components like PTCH1 and SUFU can also result in activation.

Strategies to target the Hh pathway focus on inhibiting the components that initiate the pathway including the Hh ligands, SMO, and the GLI proteins.[5] To date, targeting SMO with small molecules has been the most successful strategy. Two SMO inhibitors, vismodegib (GDC-0449) and sonidegib (LDE225),have been approved by the Food and Drug Administration(FDA) for the treatment of locally advanced basal cell carcinoma (BCC) in 2012 and 2015, respectively.[5] More recently, another SMO inhibitor, glasdegib (PF-04449913), was also approved by FDA for the treatment of acute myeloid leukemia.[6]They are currently the only drugs used clinically targeting the Hh pathway. However, drug resistance resulting from SMO mutations like SMO-D473H mutation was discovered in clinic. To overcome this problem, novel SMO inhibitors with diverse chemical structures have been developed.

Taladegib (LY2940680) (Figure 1), a phthalazine-based SMO inhibitor, is one of the few successful examples that can inhibit both the wild-type and the D473H mutant SMO in clinical trials.[7] In humans, SMO comprises three main domains including an N-terminal extracellular domain (ECD), a heptahelical membrane spanning (7-TM) domain (TMD), and a C-terminal cytoplasmic domain.[8]LY2940680 binds to a thin pocket constituted by extracellular loop protrusions and the extracellular stretch of TMD.[2]It showed weak interaction with D473, and D743H does not interfere with its binding to SMO, which contributes to its inhibitory activity towards SMO-D473H mutant.[9, 10]

Based on the binding mode of LY2940680 and SMO, compound**1** was designed and synthesized by replacing the phthalazine ring in LY2940680with anthranilamide via the ring-opening strategy (Figure 1). It displayed moderate Hh pathway inhibitory activity with IC_{50} value of 123.40 nM.

In order to improve the activity, ring A and ring B of **1** were modified using **1** as a lead compound. An initial structural modification was also made to ring C and the linker of **1**. The structures of all the new compounds were confirmed by ^{1}H-NMR, ^{13}C-NMR, and HRMS. All of these compounds were evaluated for their Hh pathway inhibitory activity. Only a few compounds showed detectable activity, and they were chosen to be evaluated for their *in vitro* proliferation inhibitory activities against

the Daoy cell line in which the Hh pathway is active. Compound **12a** exhibited the best inhibitory activity against the Hh signaling pathway (IC_{50}=34.09nM) and displayed better proliferation inhibitory activity than LY2940680.

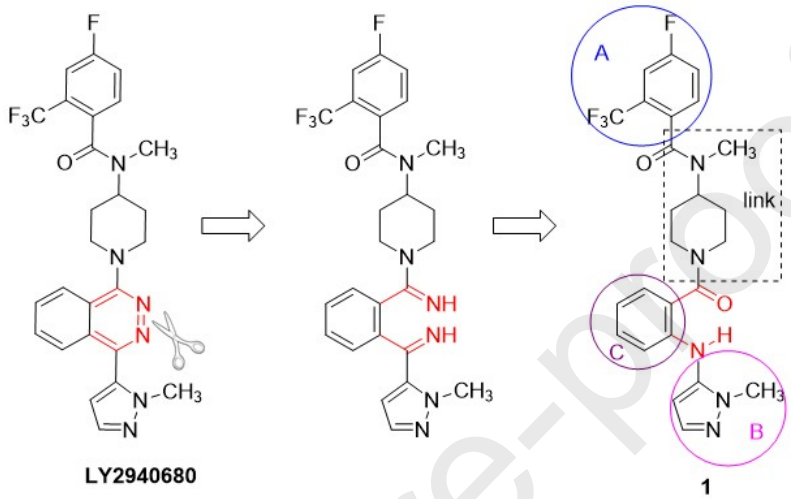

Figure 1 Use of the ring-opening strategy to obtain compound **1**.

2. Results and Discussion

2.1 Identification of the lead compound

Current understanding of the mechanism of drug resistance in SMO inhibitors suggests that mutation of aspartic acid at position 473 to histidine (D473H) is the key to the resistance of small-molecule inhibitors. To explain why the activity of LY2940680 is not affected by the D473H mutation, a re-docking of the crystal complex of LY2940680 (Figure 2A) (PDB ID: 4jkv) after virtual mutation of the amino acid was performed. The result showed that the distance between LY2940680 and the histidine at position 473 was far (4.8 Å) (Figure 2B). Therefore, the D473H mutation exhibited a weak effect on LY2940680, and this may

explain why LY2940680 is not affected by SMO (D473H) mutation. The carbonyl group of the amide in LY2940680 forms a key hydrogen bond with asparagine at position 219 (N219) in SMO to anchor LY2940680 firmly in SMO. The phenylalanine at position 484 can form a π-πstacking interaction with the 2-trifluoromethyl-4-fluoro-substituted benzene ring to maintain a stable conformation of LY2940680 in the protein. The nitrogen atom on the phthalazine ring can also form a hydrogen bond with arginine at position 400 (R400).

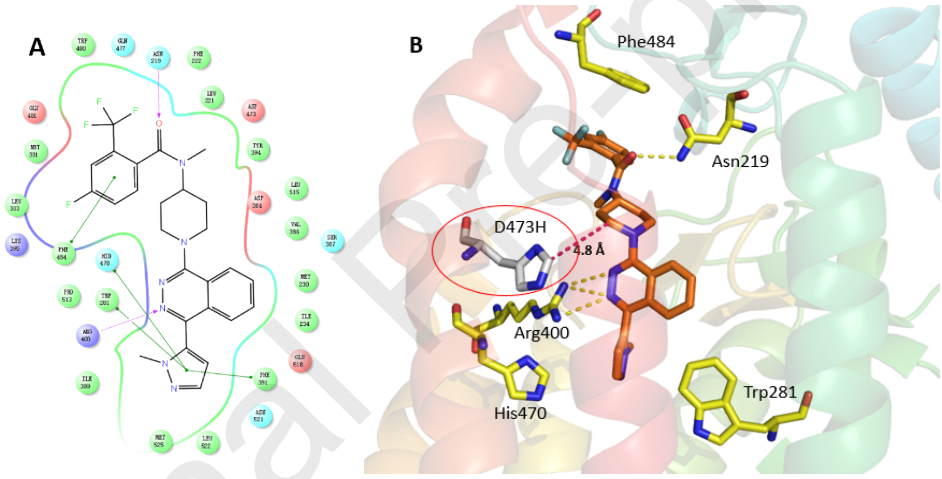

Figure 2 A: Binding mode of LY2940680 and SMO; B: D473H mutation exhibited weak effect on LY2940680 binding mode

It was assumed that the inhibitory activity towards the Hh pathway could be reserved if the molecular binding conformation was maintained. In this work, according to the principle of scaffold hopping, the phthalazine ring in LY2940680 was transformed into an anthranilamide structure by the ring-opening strategy (Figure 1).[11, 12] It was expected that the intra-molecular hydrogen bond between the carbonyl group and

the amino group could be utilized to form a pseudo-ring structure[13, 14] thus mimicking the binding conformation of LY2940680 to SMO. Moreover, the nitrogen atom in the phthalazine ring was replaced with a carbonyl group as a hydrogen bond acceptor for R400.

Changes in the structure of small molecules can change the electric properties and conformation of the entire molecule, which can affect the binding efficiency of the ligand to the receptor. Therefore, the surface electrostatic potential (ESP) of the ring-opened compound **1**was calculated using Gaussian 9.0. The results showed that the ring-opened structure in **1** had a similar ESP to the phthalazine region of LY2940680 (Figure 3) indicating that the anthranilamide structure can efficiently simulate the structure and charge distribution of the phthalazine ring.

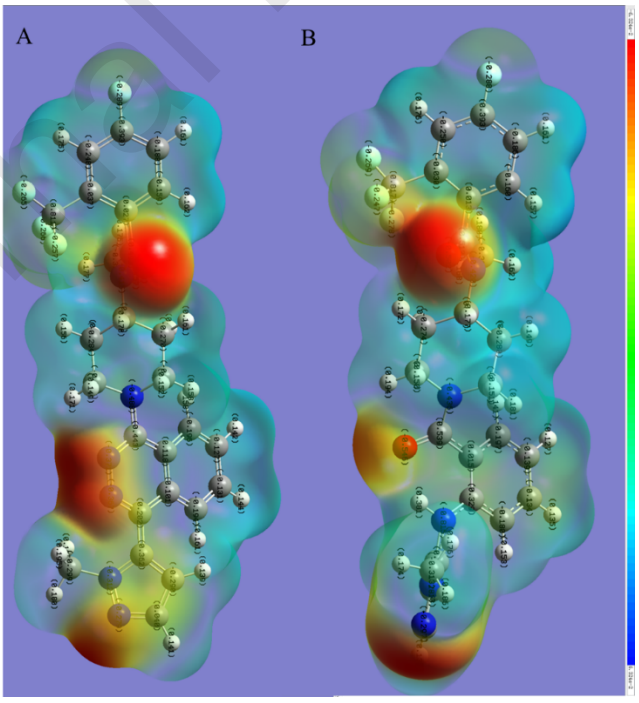

Figure 3 Surface ESP distribution (A: LY2940680; B: **1**).

Moreover, **1**was re-docked back to SMO protein (PDB ID: 4jkv) using the Glide docking program in Schrödinger2015. As shown in Figure 4A, the carbonyl group of benzamide in the ring-opened part of **1**could mimic the hydrogen bond between phthalazine ring and R400, and the carbonyl group of 2-trifluoromethyl-4-fluorobenzamide in **1** could interact with N219. When **1** overlapped on the conformation of LY2940680, a pseudo-ring structure formed by the ring-opened portion of **1** and a good superposition of **1**with LY2940680 in the pocket could be observed (Figure 4B).

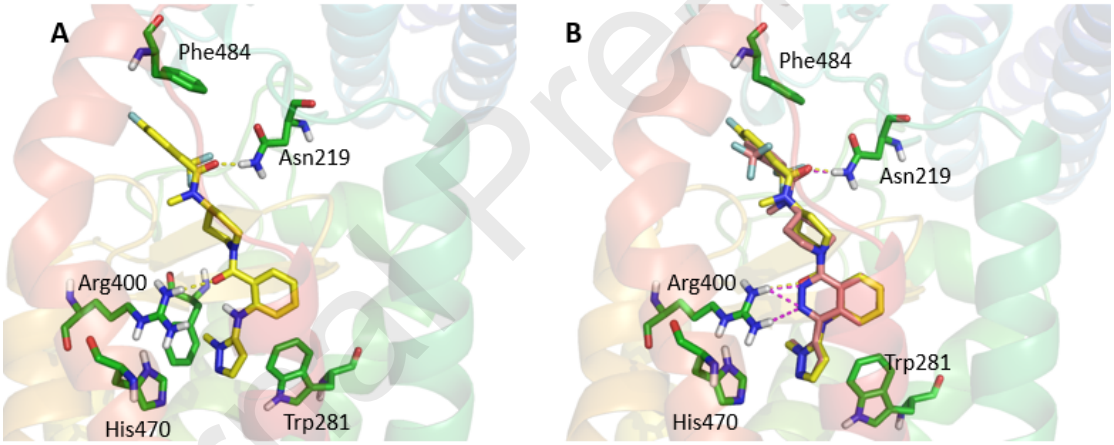

Figure 4 A: Figure of **1** docking with SMO protein; B: Plot of superposition of **1** and LY2940680 in the binding pocket (yellow: **1**, pink: LY940680).

Supported by former results, compound **1**was synthesized (scheme 1) and a dual luciferase reporter gene assay (Gli-Luciferase) was performed to measure the inhibitory activity of the compound against the Hhpathway. The results showed that **1** had inhibitory activity with an IC_{50} value of 123.40 nM, which makes it a novel lead compound although the activity was weaker than that of the positive drug LY2940680 (IC_{50} =

4.17 nM).

2.2 Synthesis and inhibitory activity on the Hh pathway

To improve the inhibitory activity, new compounds were designed and synthesized for three rounds using **1** as a lead compound. The anthranilamide derivatives were synthesized via four different routes described in Scheme1. In route 1, **3a** and **3b** were prepared by CuI mediated coupling from compound **2**. The intermediates **8a-8h** were then synthesized in three steps from compound **4** and the respective benzoic acids **6a-6h** that went through reductive amination, condensation, and deprotection. Finally, compound **1** and **9a-9g** were obtained via condensation of **3a** with **8a-8h**. In route 2, compound **10** was prepared via condensation of compound **2** and **8a**. Then compounds**12a-12i** were obtained from **10** and respective aniline**11a-11i** through a Buchward coupling reaction. In route 3, **16a** and **16b** were obtained via three steps from compound **13** with condensation, deprotection, and condensation reactions. In route 4, compound **17** was first coupled with aniline to obtain compound **18** followed by a condensation of **18** and **8a** to obtain compound **19**.

Route 1:

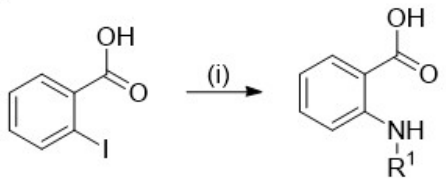

2 **3a,3b**

	R^1
3a, 16a	5-(1-methyl-1H-pyrazol-yl)
3b, 16b	phenyl

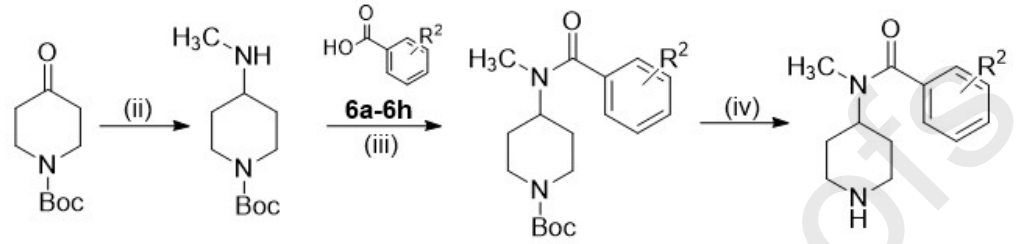

4 **5** **7a-7h** **8a-8h**

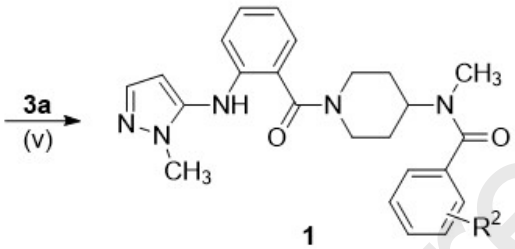

1
9a-9g

	R^2
6a, 7a, 8a, 1	2-CF_3-4-F
6b, 7b, 8b, 9a	4-NO_2
6c, 7c, 8c, 9b	4-OCH_3
6d, 7d, 8d, 9c	4-F
6e, 7e, 8e, 9d	4-CN
6f, 7f, 8f, 9e	4-CF_3
6g, 7g, 8g, 9f	4-$COCH_3$
6h, 7h, 8h, 9g	4-SO_2CH_3

Route 2:

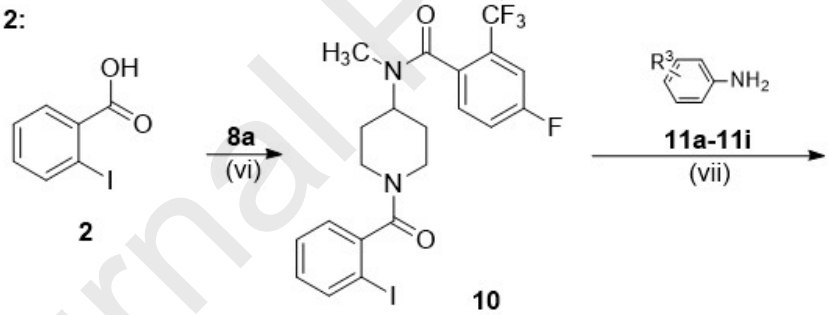

2 **10**

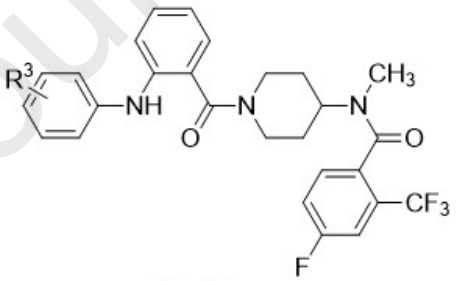

12a-12i

	R^3
11a, 12a	H
11b, 12b	4-CN
11c, 12c	2-CN
11d, 12d	4-OCH_3
11e, 12e	2-OCH_3
11f, 12f	4-pyridyl
11g, 12g	2-pyridyl
11h, 12h	4-phenyl
11i, 12i	4-COOH

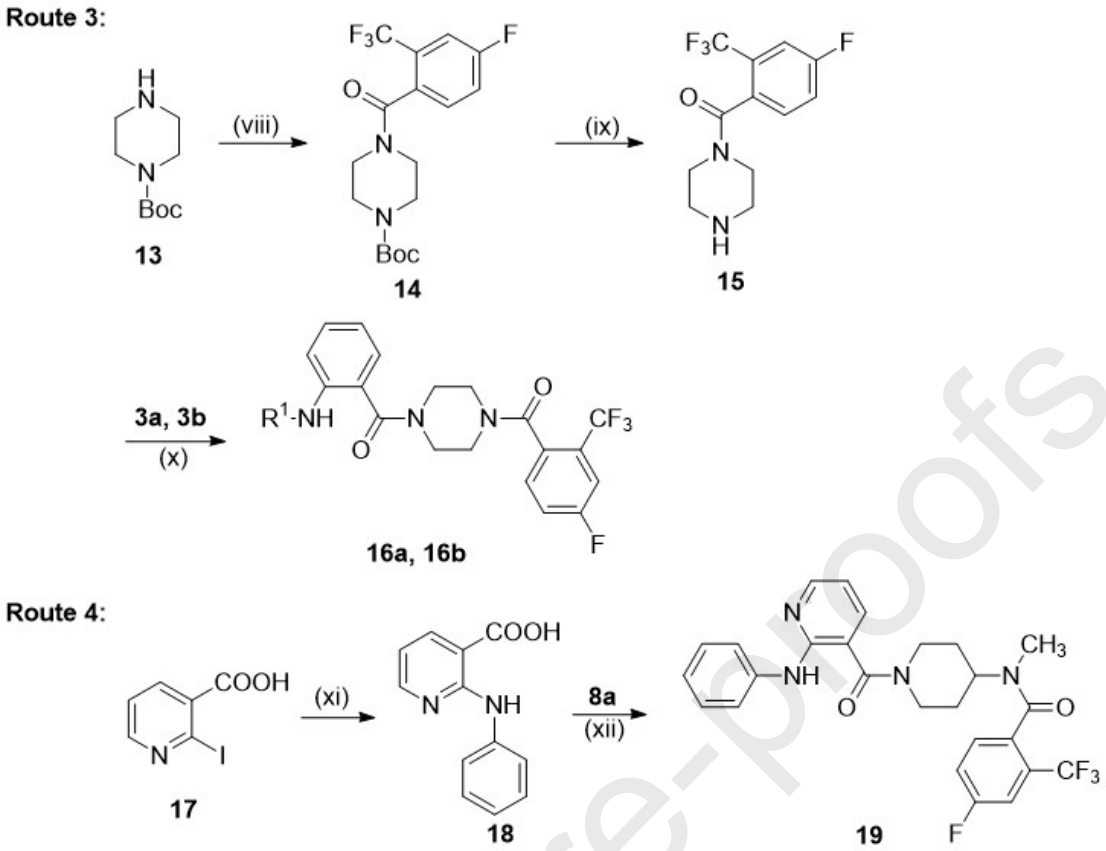

Scheme 1. Synthetic routes. Reagents and conditions: (i) anilineor1-methyl-5-amino-1H-pyrazole, CuI, K_2CO_3, DMF, 100°C, 8h, 70–72%; (ii) Methylamine, $NaBH_3CN$, MeOH, 25°C, 12h, 99%; (iii) $(COCl)_2$, Et_3N, DCM, 25°C, 1.5h, 52–91.3%; (iv) CF_3COOH, DCM, 25°C, 1.5h, 85–95%; (v) EDCI, HOBt, Et_3N, DCM, 25°C, 8h, 51–73%; (vi) $(COCl)_2$, Et_3N, DCM, 25°C, 1.5h, 86%; (vii) $Pd(OAc)_2$, BINAP, toluene, 100°C, 12h, 36-67%; (viii) 4-fluoro-2-(trifluoromethyl)benzoicacid, $(COCl)_2$, Et_3N, DCM, 25°C, 1.5h, 95%; (ix) CF_3COOH, DCM, 25°C, 1.5h, 98.4%; (x) EDCI, HOBt, Et_3N, DCM, 25°C, 8h, 62–68%; (xi) Aniline, CuI, K_2CO_3, DMF/H_2O, 100°C, 8h, 94%; and (xii) EDCI, HOBt, Et_3N, DCM, 25°C, 8h, 59%.

First, the substituents on ring A of **1** were replaced to obtain compounds **9a-9g**, and they were subjected to the dual luciferase reporter gene assay. The activities of these compounds were greatly reduced, and some of them even lost the inhibitory activity against the Hh pathway

(Table 1).

Table 1 Inhibitor activity of compounds **9a-9g**against the Hh pathway (n = 2).

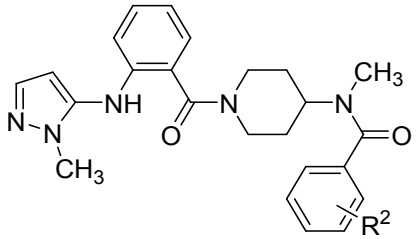

Compound	R^2	Gli-Luciferase reporter IC_{50}(nM)
9a	4-NO_2	308.7 ± 73.1
9b	4-OCH_3	561.9 ±185.9
9c	4-F	>10000
9d	4-CN	4365.5 ±1130.7
9e	4-CF_3	1328.0 ±131.5
9f	4-$COCH_3$	1909.5 ±262.3
9g	4-SO_2CH_3	>10000
LY2940680		4.56 ±0.33
Vismodegib		13.06 ±0.44

The first round of optimization showed that the activity was considerably reduced or even removed after the substituents of ring A of **1** were replaced. This preliminary result indicated that 2-trifluoromethyl-4-fluorophenyl is the key pharmacophore. It can form non-polar interactions with multiple amino acids (M301, K395, W480, E481, F484, and P513) in the extracellular ligand-binding domain of SMO, which makes it important to maintain the activity.

In further structural modifications, the 2-trifluoromethyl-4-fluorophenyl structure of ring A was retained, and

ring B was replaced with different substituted benzene rings to obtain compounds **12a-12i**. These compounds were also subjected to the dual luciferase reporter gene assay, and the results showed that the activity was improved when the benzene ring was not substituted (IC_{50} = 34.09nM, which is higher than that of **1**by 3-fold). The activities of the remaining compounds containing other substituents showed a large decline (Table 2).

Table 2 Inhibitor activity of compounds **12a-12i** against the Hh pathway (n = 2).

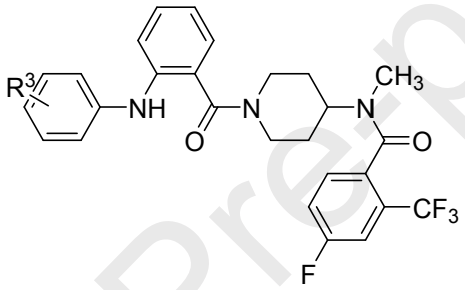

Compound	R^3	Gli-Luciferase reporter IC_{50} (nM)
12a	H	34.09 ±1.60
12b	4-CN	6864 ±315.4
12c	2-CN	9369.5 ±125.1
12d	4-OCH_3	754.05 ±17.32
12e	2-OCH_3	285.25 ±126.6
12f	4-pyridyl	>10000
12g	2-pyridyl	>10000
12h	4-phenyl	4858.0 ±557.2
12i	4-COOH	>10000
LY2940680		7.64 ±0.21
Vismodegib		21.87±1.98

Finally, the linker of the most active compounds **1** and **12a** were shortened to obtain compounds**16a** and **16b**, and the benzene ring in ring C of **12a**wasreplaced with a pyridine ring to obtain compound **19**. However, the results of the dual luciferase reporter gene assay showed that the activities of the modified compounds were significantly decreased (**16a** and **16b**: IC_{50}> 10000 nM; **19**: IC_{50} = 7117 nM).

2.3 Molecular dynamics simulation analysis

The compounds obtained via the ring-opening strategy showed a decrease in the inhibitory activities against the Hh pathway comparing with LY2940680.The causes of the decline in the inhibitory activities against the Hh pathway was next explained from a molecular perspective.

First, a molecular dynamics simulation (4 ns) of LY2940680 and **12a**was performed using Discovery studio 2.5. Throughout the simulation, the root-mean-square deviations (RMSD) of the system relative to the initial structure were used to investigate the dynamic stability of the system and to ensure the rationality of the dynamic sampling. Figure5 shows that both systems reached equilibrium after 2 ns.

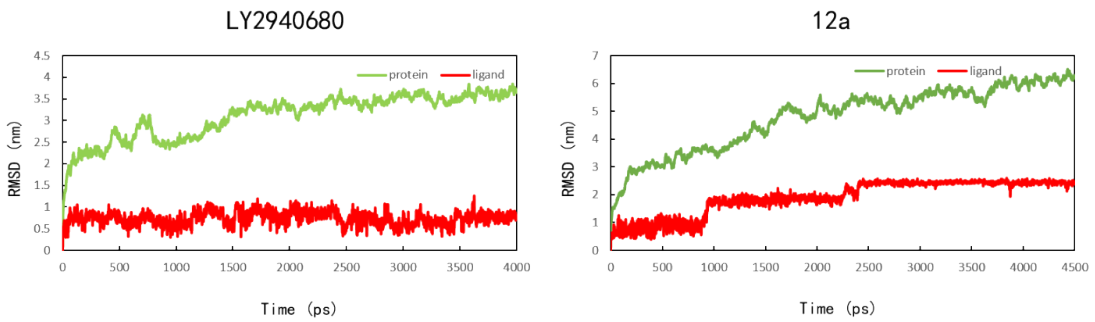

Figure 5 RMSD values of the backbone of the LY2940680-SMO complex and the **12a**-SMO complex during molecular dynamics simulations.

The dynamic trajectory in the last 1 ns of the whole simulation process was subsequently selected and the number of hydrogen bonds were separately calculated (Figure 6). The results showed that the average number of hydrogen bonds in the LY2940680-SMOcomplex was 2.60, which is more than the value of 1.50 in the **12a**-SMO complex. A conformation at every 10 ps in the last 1 ns of the dynamic trajectory was then selected to calculate the average conformation (Figure 7). Although**12a** could form hydrogen bonds with ARG400, the average distance was 0.31 ± 0.03 nm. LY2940680 could form two hydrogen bonds with ARG400, and the average distances were 0.21 ± 0.01 nm and 0.27 ± 0.02 nm. In addition, **12a** migrates to the lower part of SMO causing a large spatial deviation of the entire molecule from LY2940680. As a result, the segment of 2-trifluoromethyl-4-fluorobenzamide in **12a** cannot form a hydrogen bond with ASN219, and the activity is reduced.

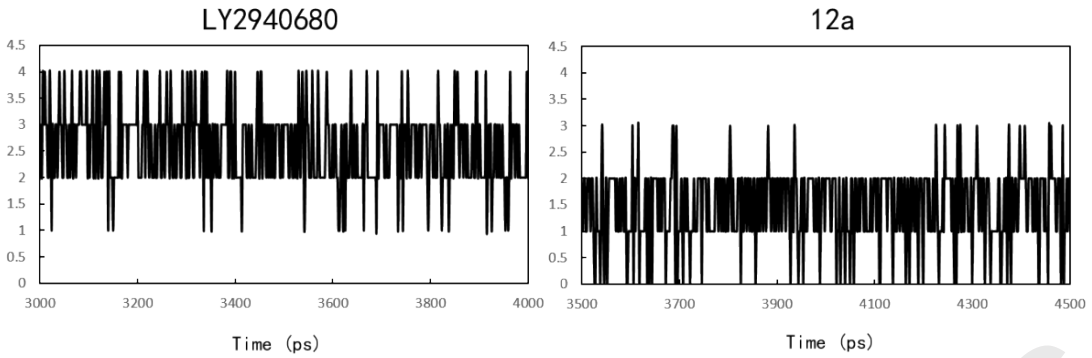

Figure 6 Hydrogen bond numbers of the LY2940680-SMO complex and the **12a**-SMO complex via molecular dynamics simulations.

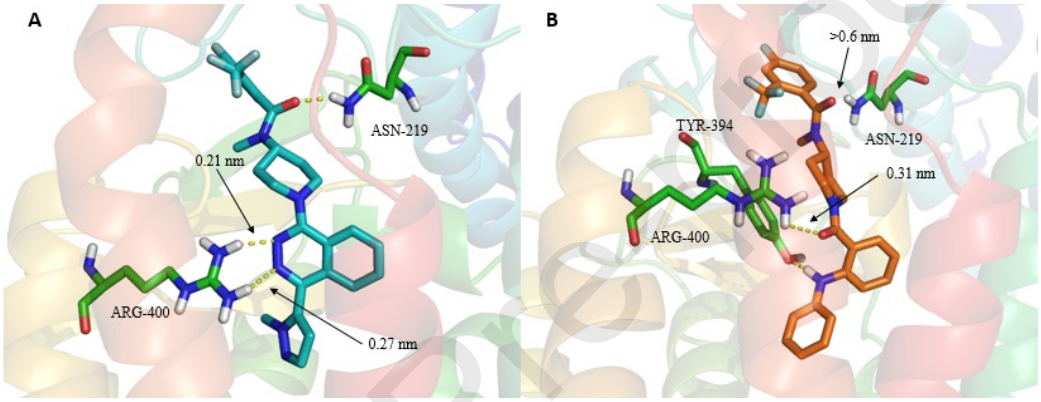

Figure 7Average conformations of (A) LY2940680-SMO complex and (B) **12a**-SMO complex.

The binding free energy ΔG of LY2940680 and **12a**wasalso calculated using QM-Polarized Ligand Docking (QPLD) combined with Prime-MM/GBSA (Table 3).

$\Delta G_{bind} = G_{complex} - (G_{protein} + G_{ligand}) = \Delta G_{MM} + \Delta G_{sol} - T\Delta S$,where$\Delta G_{MM} = \Delta G_{ele} + \Delta G_{vdW}$, $\Delta G_{sol} = \Delta G_{polar} + \Delta G_{nonpolar}$.

The calculation results show that the binding free energies of LY2940680 and **12a**were negative (the influence of entropy change was ignored here). This is due to several reasons. First, whenthe ring in LY2940680 is opened, there will inevitably be an increase in entropy depletion for the binding process to compensate for increasing degree of

freedom caused by multiple conformations—this increases the ΔG.[15] Second, the current entropy change calculation is greatly affected by the definition of degree of freedom. There are high requirements for the computing capability of computers—especially when macromolecules are involved; thus, the precision is relatively low. Therefore, the influence of entropy change was ignored. This result indicated that both LY2940680 and **12a** could interact strongly with SMO. The binding free energy of LY2940680 was lower than that of **12a** indicating that LY2940680 has a higher affinity for the SMO binding pocket, which also explains the difference between the activity of **12a** and that of LY2940680. This study may provide additional references for designing SMO inhibitors using computational principles in the future.

Table 3 Calculation of binding free energy via the MM/GBSA method.

	LY2940680(kJ/mol)	**12a**(kJ/mol)
ΔE_{vdw}	-75.416	-72.455
ΔE_{ele}	-43.737	-38.807
ΔG_{polor}	55.188	54.364
$\Delta G_{nonpolor}$	11.769	11.910
ΔG_{bind}	-52.196	-44.988

2.4 Proliferation inhibitory activity

Compounds **1**, **9a**, **12a**, and **12e** with relatively strong inhibitory activity against the Hh pathway were further selected to measure their *in vitro* proliferation inhibitory activities. Since the Hh pathway is activated

in medulloblastoma[16], the human medulloblastoma cell line Daoy was chosen for *in vitro* anti-proliferative activity tests. The results are shown in Table 4. The results showed that the tested compounds exhibited strong proliferation inhibitory activities towards Daoy cells with IC_{50} values ranging from 0.40 μM to 0.87 μM; compounds **1**, **12a**, and **12e**displayed better activity than the positive control LY2940680.

In comparison, the anti-proliferative activities of these compounds towards the human melanoma cell line A2058 were also investigated. This cell line has been known for the over-activation of the MAP kinase pathway resulting from the BRAF V600E mutation [17]. The results showed that all the tested compounds displayed very poor inhibitory activities with IC_{50} values more than 50 μM. This indicates that these potential SMO inhibitors may selectively inhibit the proliferation of the cancer cells that depend on the Hh pathway.

Table 4Anti-proliferative activities of the tested compounds on the human medulloblastoma cell line Daoy (n = 3).

Compound	IC_{50} (μM)
1	0.51 ± 0.05
9a	0.87 ± 0.09
12a	0.48 ± 0.05
12e	0.40 ± 0.02
LY2940680	0.79 ± 0.06

3. Conclusion

Mutations of SMO, like SMO (D473H) mutant, can result in drug

resistance in clinical treatment. LY2940680 is one of the few drugs that are active to both wild-type and D473H mutant SMO. In this work, a novel compound **1**with similar electrical property to LY2940680 was designed by a ring-opening strategy based on the binding mode of LY2940680 and SMO. The phthalazine ring in LY2940680was replaced with anthranilamide. The Glide docking study suggested that the anthranilamide in **1** can form a pseudo-ring structure and its carbonyl group can mimic the hydrogen bond between the phthalazine ring and R400 of SMO, which supported this design. As expected, compound **1** displayed a moderate inhibitory activity towards the Hh pathway (IC_{50} = 123.40 nM). To improve the activity, three rounds of structural modification have been made, and compound **12a** displayed the most promising activity with an IC_{50} value of34.09nM, which is still less active than LY2940680 (IC_{50} = 7.64 nM).The weaker hydrogen bond with SMO and higher binding free energy might be responsible for the lower activity as supported by the molecular dynamics analysis. Compound **12a** exhibited a higher proliferation inhibitory activity towards the human medulloblastoma cell line Daoy than LY2940680, indicating an alternative mechanism of the anticancer action. Studies into the mechanism are ongoing.

4. Experimental Section

4.1 Chemistry

4.1.1 General

Unless otherwise stated, all reagents were purchased from commercial suppliers and used without purifications. ^{1}H NMR and ^{13}C NMR spectra were obtained on a Bruker AV-300 nuclear instrument in $CDCl_3$ or DMSO-d_6 using TMS as internal standard, operating at 300 MHz and 75 MHz, respectively. Chemical shifts (δ) are expressed in ppm and coupling constants J are given in Hz. Analytical thin layer chromatography (TLC) was performed on pre-coated, glass-backed silica gel plates. Visualization of the developed chromatogram was performed by UV absorbance (254 nm). High resolution mass spectra (HRMS) were obtained on a Waters Q-TOF micro TM apparatus. Melting points were measured with an RY-I melting point apparatus.

4.1.2Synthesis

2-((1-Methyl-1H-pyrazol-5-yl) amino) benzoic acid (3a)

To a mixture of 2-iodobenzoic acid (5.00 g, 20.00 mmol), 1-methyl-5-amino-1H-pyrazole (1.90 g, 20.00 mmol) and Potassium carbonate (5.50 g, 40.00 mmol) in 20 mL DMF were added CuI (0.76 g, 4.00 mmol). The reaction mixture was stirred at 105 ^{o}C for 8 h. After cooling to room temperature the mixture was poured into 60 ml water and the pH was adjusted to 5-6 using 1N HCl. The formed precipitates were filtrated and dried to obtained black solid. Yield: 70%, m.p. 134~139 ^{o}C.^{1}H-NMR (300 MHz, $CDCl_3$) δ (ppm):10.77-8.78 (m, 2H, NH, ArH),

8.14-7.30(m, 3H, ArH), 6.89 (s, 1H, ArH), 6.46(s, 1H, ArH), 3.85(s, 3H, CH_3).

2-(Phenylamino) benzoic acid (3b)

To a mixture of 2-iodobenzoic acid (5.00 g, 20.00 mmol), Aniline (1.86 g, 20.00 mmol) and Potassium carbonate (5.50 g, 40.00 mmol) in 20 mL DMF were added CuI (0.76 g, 4.00 mmol).The reaction mixture was stirred at 105 ^oC for 8 h. After cooling to room temperature the mixture was poured into 60 mL water and the pH was adjusted to 4~5 using 1N HCl.The formed precipitates were filtrated and dried to obtained yellow solid. Yield: 72%,m.p. 180~182 ^oC.^{1}H-NMR (300 MHz, $CDCl_3$) δ (ppm): 9.31 (brs, 1H, COOH), 8.05 (d, J = 8.10 Hz, 1H, ArH), 7.40-7.33 (m, 3H, ArH), 7.29-7.21 (m, 3H, ArH), 7.16-7.11 (m, 1H, ArH), 6.78-6.73 (m, 1H, ArH).

Tert-butyl-4-(methylamino) piperidine-1-carboxylate (5)

A mixture of tert-butyl 4-oxopiperidine-1-carboxylate (1.00 g, 5.00 mmol) Methylamine (10.00 mL) in 5mlMeOH was adjusted to pH=5-6 with acetic acid and stirred under room temperature for 1 h. Then cooling to 0 ^oC and $NaBH_3CN$ (0.48 g, 7.60 mmol) was added portion wise. The mixture was stirred under room temperature for 12h until the reaction was complete. The methanol was evaporated under reduced pressure then the pH was adjusted to 9 with 1N NaOH. The mixture was extracted with DCM, dried with Sodium sulphate. The solvent was evaporated to obtain

the yellow oil, Yield: 100%. ^{1}H-NMR (300 MHz, CDCl3) δ (ppm): 3.98 (d, J = 10.20 Hz, 2H, Boc-NCH_2), 2.74 (t, J = 12.20 Hz, 2H, BocNCH_2), 2.48-2.43(m, 1H, NHCH), 2.38 (s, 3H, $NHCH_3$), 1.79 (d, J = 12.20 Hz, 2H, $NHCHCH_2$), 1.39 (s, 9H, Boc-H), 1.17 (dd, J = 20.20, 10.20 Hz, 2H, $NHCHCH_2$).

General procedures for the synthesis of 7a-7h

The purchased acids (14.40 mmol) was added into 5 mL DCM and cooled to 0 ^{o}C.After the oxalyl chloride (1.50 mL,17.30 mmol) was added drop wise, the mixture was removed to room temperature and stirred for 30min. The solvent was evaporated for use.

To a cooled solution of **5** (3.70 g，17.30 mmol) in 20 mL DCM was added Et_3N (3.00 mL， 21.60 mmol) then the prepared chloride was added drop wise. The mixture was stirred at room temperature for 1 h. The solvent was evaporated under reduced pressure and the residue was purification by column chromatography with dichloromethane/ methanol as eluent on silica gel to give the derivatives**7a**-**7h**.

Tert-butyl-4-(4-fluoro-N-methyl-2-(trifluoromethyl) benzamido) piperidine-1-carboxylate (7a)

Colorless oil, yield: 91.3%. Major rotamer: ^{1}H-NMR (300 MHz, $CDCl_3$) δ (ppm): 7.44-7.39 (m, 1H, ArH), 7.32-7.29 (m, 2H, ArH), 4.73 (m, 1H, CH3NCH), 4.25 (m, 2H, BocNCH_2), 2.88-2.82 (m, 2H, BocNCH_2), 2.63 (s, 3H, NCH_3), 1.79-1.63 (m, 4H, $CH_3N(CH_2)_2$), 1.46 (s, 9H,

Boc-H).Minor rotamer: ^{1}H-NMR (300 MHz, $CDCl_3$) δ (ppm): 7.44-7.39 (m, 1H, ArH), 7.32-7.29 (m, 2H, ArH), 4.15-4.11 (m, 2H, $BocNCH_2$), 3.23 (s, 1H, CH_3NCH), 2.98 (s, 3H, NCH_3), 2.51-2.35 (m, 2H, $BocNCH_2$), 1.79-1.63 (m, 4H, $CH_3N(CH_2)_2$), 1.43 (s, 9H, Boc-H).

Tert-butyl-4-(N-methyl-4-nitrobenzamido) piperidine-1-carboxylate (7b)

Yellow solid, yield: 82%, m.p. 152~153 ^{o}C.^{1}H-NMR (300 MHz, $CDCl_3$) δ (ppm): 8.31 (d, J = 7.90 Hz, 2H, ArH), 7.58 (d, J = 7.20 Hz, 2H, ArH), 4.72 (s, 1H, CONCH), 4.26 (brs, 2H, $CONCHCH_2$), 3.01 (brs, 2H, $CONCHCH_2$), 1.77 (s, 3H, $CONCH_3$), 1.49 (brs, 4H, $BocN(CH_2)_2$), 1.49(s, 9H, Boc-H).

Tert-butyl-4-(4-methoxy-N-methylbenzamido)piperidine-1-carboxylate (7c)

White solid, yield: 88%, m.p. 116~117 ^{o}C.^{1}H-NMR (300 MHz, $CDCl_3$) δ (ppm):7.39 (d, J = 8.50 Hz, 2H, ArH), 6.94 (d, J = 8.60 Hz, 2H, ArH), 4.62 (brs, 1H, CONCH), 4.25-4.21 (m, 2H, $CONCHCH_2$), 3.87 (s, 3H, OCH_3), 2.91 (s, 3H, NCH_3), 2.77 (brs, 1H, $ONCHCH_2$), 1.73 (brs, 4H, $BocN(CH_2)_2$), 1.51 (s, 9H, Boc-H).

Tert-butyl-4-(4-fluoro-N-methylbenzamido) piperidine-1-carboxylate (7d)

Yellow oil, yield: 76%. ^{1}H-NMR (300 MHz, $CDCl_3$) δ (ppm):7.53-7.34 (m, 2H, ArH), 7.15-7.08 (m, 2H, ArH), 4.67 (s, 1H, CONCH), 4.23 (s,

2H, $CONCHCH_2$), 3.27-3.00 (m, 2H, $CONCHCH_2$), 2.88 (s, 3H, NCH_3), 1.72 (brs, 4H, $ONCHCH_2$), 1.49 (s, 9H, Boc-H).

Tert-butyl-4-(4-cyano-N-methylbenzamido) piperidine-1-carboxylate (7e)

White solid, yield: 71%, m.p. 120~121 ^oC.^{1}H-NMR (300 MHz, $CDCl_3$) δ (ppm):7.76 (d, J = 8.00 Hz, 2H, ArH), 7.51 (d, J = 7.30 Hz, 2H, ArH), 4.71 (s, 1H， CONCH), 4.27 (brs, 2H, $CONCHCH_2$), 3.00-2.89 (m, 1H, $CONCHCH_2$), 2.81 (s, 3H, NCH_3), 2.51 (s, 1H, $CONCHCH_2$), 1.77-1.71 (m, 4H, $BocN(CH_2)_2$), 1.50 (s, 9H, Boc-H).

Tert-butyl-4-(N-methyl-4-(trifluoromethyl)benzamido) piperidine-1-carboxylate (7f)

White solid, yield: 70%, m.p. 122~123 ^oC.^{1}H-NMR (300 MHz, $CDCl_3$) δ (ppm):7.71 (d, J = 8.00 Hz, 2H, ArH), 7.52 (d, J = 7.60 Hz, 2H, ArH), 4.73 (s, 1H, CONCH), 4.27 (s, 2H, $CONCHCH_2$), 3.00 (s, 1H, $CONCHCH_2$), 2.81 (s, 3H, NCH_3), 2.52 (s, 1H, $CONCHCH_2$), 1.77 (brs, 4H, $BocN(CH_2)_2$), 1.49 (s, 9H, Boc-H).

Tert-butyl-4-(4-acetyl-N-methylbenzamido) piperidine-1-carboxylate (7g)

Yellow solid, yield: 52%, m.p. 101~102 ^oC.^{1}H-NMR (300 MHz, $CDCl_3$) δ (ppm):8.02 (d, J = 8.10 Hz, 2H, ArH), 7.48 (d, J = 7.60 Hz, 2H, ArH), 4.72 (s, 1H, CONCH), 4.25 (brs, 2H, $CONCHCH_2$), 2.94-2.89 (m, 1H, $CONCHCH_2$), 2.80 (s, 3H, NCH_3), 2.64 (s, 3H, $COCH_3$), 2.50-2.43 (m,

1H, CONCHCH$_2$), 1.76 (brs, 4H, BocN(CH$_2$)$_2$), 1.48 (s, 9H, Boc-H).

Tert-butyl-4-(N-methyl-4-(methylsulfonyl) benzamido) piperidine-1-carboxylate (7h)

White solid, yield: 69%, m.p. 196~197^{o}C.^{1}H-NMR (300 MHz, CDCl$_3$) δ (ppm):8.01 (d, J = 8.10 Hz, 2H, ArH), 7.57 (d, J = 7.40 Hz, 2H, ArH), 4.69 (m, 1H, CONCH), 4.44-4.00 (m, 2H, CONCHCH$_2$), 3.07 (s, 3H, SO$_2$CH$_3$), 3.03-2.81 (m, 2H, CONCHCH$_2$), 2.77 (s, 3H, NCH$_3$), 1.85-1.60 (m, 4H, BocN(CH$_2$)$_2$), 1.46 (s, 9H, Boc-H).

General procedures for the synthesis of 8a-8h

To a solution of **7a-7h** (10.70 mmol) in 20 mL DCM was added 5 mL TFA the stirred at room temperature for 1h. The solvent was evaporated under reduced pressure and the residue was used without further purification.

Tert-butyl 4-(4-fluoro-2-(trifluoromethyl) benzoyl) piperazine-1-carboxylate (14)

4-Fluoro-2-(trifluoromethyl)benzoic acid (3.00 g, 14.40 mmol) was added into 5 mL DCM and cooled to 0 ^{o}C.After the oxalyl chloride (1.50 mL, 17.30 mmol) was added drop wise, the mixture was removed to room temperature and stirred for 30min. The solvent was evaporated for use.

To a cooled solution of tert-butyl piperazine-1-carboxylate (3.20 g，17.30 mmol) in 20 mL DCM was added Et$_3$N (3.00 Ml，21.60 mmol) then the prepared chloride was added drop wise. The mixture was stirred at room

temperature for 1 h. The solvent was evaporated under reduced pressure and the residue was purification by column chromatography on silica gel to give the colorless oil, yield: 95%.

(4-Fluoro-2-(trifluoromethyl) phenyl) (piperazin-1-yl) methanone (15)

To a solution of **14**(5.13 g, 13.60 mmol) in 20 mL DCM was added 5 ml TFA the stirred at room temperature for 1h. The solvent was evaporated under reduced pressure and the residue was purification by column chromatography on silica gel to give the yellow oil, yield: 98.4%. ^{1}H-NMR (300 MHz, $CDCl_3$) δ (ppm):7.37 (dd, J = 8.70, 1.90 Hz, 1H, ArH), 7.33-7.20 (m, 2H, ArH), 3.94-3.49 (m, 2H, piperazine-H), 3.10 (t, J = 5.00 Hz, 2H, piperazine-H), 2.88 (t, J = 5.10 Hz, 2H, piperazine-H), 2.80-2.59 (m, 2H, piperazine-H).

4-Fluoro-N-(1-(2-iodobenzoyl) piperidin-4-yl)-N-methyl-2-(trifluoromethyl) ben-zamide (10)

2-Iodobenzoic acid(2.00 g, 8.00 mmol) was added into 10 mL DCM and cooled to 0 ^{o}C.After the oxalyl chloride (0.80 mL，9.60 mmol) was added drop wise, the mixture was removed to room temperature and stirred for 30min. The solvent was evaporated for use.

To a cooled solution of **8a** (2.40 g, 8.00 mmol) in 20 mL DCM was added Et_3N (1.70 mL, 12.00 mmol) then the prepared chloride was added drop wise. The mixture was stirred at room temperature for 1 h. The solvent

was evaporated under reduced pressure and the residue was purification by column chromatography with dichloromethane/ methanolas eluent on silica gel to give the yellow solid, yield: 86%, m.p. 85~86 ^{o}C. Major rotamer: ^{1}H-NMR (300 MHz, $CDCl_3$) δ (ppm): 7.91-7.81 (m, 1H, ArH), 7.45-7.36 (m, 2H, ArH), 7.36-7.28 (m, 2H, ArH), 7.24-7.17 (m, 1H, ArH), 7.14-7.02 (m, 1H, ArH), 5.00-4.75 (m, 1H, CH_3NCH), 4.23 (brs, 2H, $NCHCH_2$), 3.07 (br, 2H, $NCHCH_2$), 2.58(s, 3H, CH_3), 1.75 (m, 4H, $CON(CH_2)_2$). Minor rotamer: ^{1}H-NMR (300 MHz, $CDCl_3$) δ (ppm): 7.91-7.81 (m, 1H, ArH), 7.45-7.36 (m, 2H, ArH), 7.36-7.28 (m, 2H, ArH), 7.24-7.17 (m, 1H, ArH), 7.14-7.02 (m, 1H, ArH), 4.23 (brs, 2H, $NCHCH_2$), 3.38(m, 1H, CH_3NCH), 3.02 (s, 3H, CH_3), 2.41(brs, 2H, $NCHCH_2$), 1.75 (m, 4H, $CON(CH_2)_2$).

2-(Phenylamino) nicotinic acid (18)

To a mixture of 2-iodonicotinic acid (5.00 g, 20.00 mmol), aniline (1.86 g, 20.00 mmol) and Potassium carbonate (5.50 g, 40.00 mmol) in 20 mL DMF were added CuI (0.76 g, 4.00 mmol). The reaction mixture was stirred at 105 ^{o}C for 8 h. After cooling to room temperature the mixture was poured into 60 mL water and the pH was adjusted to 5~6 using 2N HCl. The formed precipitates were filtrated and dried to obtained yellow solid, yield: 94%, m.p. 183~184 ^{o}C.^{1}H-NMR (300 MHz, $CDCl_3$) δ (ppm):10.08 (s, 1H, COOH), 8.49-8.37 (m, 1H, ArH), 8.33 (d, J = 7.70 Hz, 1H, ArH), 7.64 (d, J = 7.90 Hz, 2H, ArH), 7.36 (t, J = 7.40 Hz, 2H,

ArH), 7.10 (t, J = 7.40 Hz, 1H, ArH), 6.88-6.57 (m, 1H, ArH), 5.38(brs, 1H, NH).

General procedure for the synthesis of 1, 9a-9g, 16a, 16b, 19

To a mixture of**3a**(500.00 mg, 2.30 mmol) and **8a**-**8h**, **15** (2.3 mmol) in 20 mL DCM was added HoBt (372.00 mg, 2.76 mmol) then EDCI (530.00 mg, 2.76 mmol) was added portion wise. After the reaction was complete, solvent was evaporated under reduced pressure and the residue was purification by column chromatography with dichloromethane/ methanol as eluent on silica gel to give the compounds **1**, **9a-9g**, **16a**, **16b**, **19**.

N-methyl-N-(1-(2-((1-methyl-1H-pyrazol-5-yl) amino) benzoyl) piperidin-4-yl)-2-trifluoromethyl-4-fluoro-benzamide (1)

Green solid, yield: 64%, m.p. 206~207 ^{o}C. Major rotamer: ^{1}H-NMR (300 MHz, $CDCl_3$) δ (ppm): 7.47-7.41(m, 2H, ArH), 7.34-7.29 (m, 3H, ArH), 7.27-7.12 (m, 2H, ArH, NH), 6.91-6.75 (m, 2H, ArH), 6.06(s, 1H, ArH), 5.00-4.81 (m, 1H, CH_3NCH), 4.80-4.12 (m, 2H, $CON(CH_2)_2$), 3.72 (s, 3H, CH_3), 3.29-3.03 (m, 2H, $CON(CH_2)_2$), 2.67(s, 3H, CH_3), 1.84 (m, 4H, $NCH(CH_2)_2$).Minor rotamer: ^{1}H-NMR (300 MHz, $CDCl_3$) δ (ppm): 7.47-7.41(m, 2H, ArH) 7.34-7.29 (m, 3H, ArH), 7.27-7.12 (m, 2H, ArH), 6.91-6.75 (m, 2H, ArH), 6.06(s, 1H, ArH), 4.80-4.12 (m, 2H, $CON(CH_2)_2$), 3.70 (s, 3H, CH_3), 3.43-3.60 (m, 1H, CH_3NCH), 3.02 (s, 3H, CH_3), 2.64-2.55 (m, 2H, $CON(CH_2)_2$), 1.84 (m, 4H,

NCH(CH_2)$_2$).Major rotamer: ^{13}C-NMR (75 MHz, $CDCl_3$) δ (ppm): 169.54, 167.52, 161.65 (d, J = 251.50 Hz), 143.59, 138.09, 130.89, 128.91, 128.80, 128.50, 128.40, 127.68, 122.30 (q, J = 276.20 Hz), 119.18, 118.65 (d, J = 36.10 Hz), 118.47, 114.64, 113.95 (ddd, J = 25.30, 9.20, 4.70 Hz), 98.11, 50.54, 34.46, 31.11, 28.64, 27.95.Minor rotamer: ^{13}C-NMR (75 MHz, $CDCl_3$) δ (ppm): 169.54, 167.52, 161.65 (d, J = 251.50 Hz), 143.59, 138.09, 131.02, 128.91, 128.80, 128.50, 128.40, 127.54, 122.30(q, J = 276.20 Hz), 119.18, 118.65(d, J = 36.10 Hz), 118.47, 114.64, 113.95 (ddd, J = 25.30, 9.20, 4.70 Hz), 98.25, 56.13, 34.46, 29.41, 28.99, 27.02.HRMS (ESI): m/z $[M+H]^+$. Calcd for $C_{25}H_{26}F_4N_5O_2$: 504.2023; found 504.2008.

N-(1-(2-((1-methyl-1H-pyrazol-5-yl) amino) benzoyl) piperazin-4-yl)-2-trifluoro-methyl-4-fluoro-benzamide (16a)

Gray solid, yield: 68%, m.p. 84~85 ^{o}C.^{1}H-NMR (300 MHz, $CDCl_3$) δ (ppm): 7.38-7.35 (m, 2H, ArH), 7.27-7.26 (m, 2H, ArH), 7.20-7.15 (m, 2H, ArH, NH), 7.10 (d, J = 7.60 Hz, 1H, ArH), 6.76 (t, J = 7.4 Hz, 1H, ArH), 6.71 (d, J = 8.30 Hz, 1H, ArH), 5.95 (s, 1H, ArH), 3.95-3.87 (m, 1H, piperazine-H), 3.85-3.72 (m, 1H, piperazine-H), 3.68-3.63 (m, 3H, piperazine-H), 3.62 (s, 3H, CH3), 3.54-3.44 (m, 1H, piperazine-H), 3.20-3.19 (m, 2H, piperazine-H). ^{13}C-NMR (75 MHz, $CDCl_3$) δ (ppm): 169.90, 166.22, 161.89 (d, J = 252.40 Hz), 143.96, 138.10, 131.34, 129.82 (dd, J = 4.50, 2.30 Hz), 129.09, 129.02, 128.98, 127.80, 123.73 (q,

J = 233.60 Hz), 119.12 (d, J = 21.40 Hz), 118.46, 118.08, 114.63, 114.16 (dd, J = 24.80, 4.50 Hz), 98.23, 46.64, 41.54, 34.50.HRMS (ESI): m/z $[M+H]^+$. Calcd for $C_{23}H_{22}F_4N_5O_2$: 476.1710; found 476.1699.

N-methyl-N-(1-(2-((1-methyl-1H-pyrazol-5-yl) amino) benzoyl) piperidin-4-yl)-4-nitrobenzamide (9a)

Yellow solid, yield: 62%, m.p.91~92 °C.^{1}H-NMR (300 MHz, $CDCl_3$) δ (ppm): 8.31 (d, J = 8.40 Hz, 2H, ArH), 7.58 (d, J = 8.40 Hz, 2H, ArH), 7.47 (s, 1H, ArH), 7.30-7.16 (m, 3H, ArH, NH), 6.90-6.81 (m, 2H, ArH), 6.04 (s, 1H, ArH), 4.85 (s, 1H, CH_3NCH), 4.69-4.30(m, 2H, $CONCH_2$), 3.73 (s, 3H, CH_3), 3.14-3.01 (m, 2H, $CONCH_2$), 2.84 (s, 3H, CH_3), 1.89-1.74 (m, 4H, $CONCH(CH_2)_2$). ^{13}C-NMR (75 MHz, $CDCl_3$) δ (ppm): 170.06, 169.34, 148.38, 144.18, 142.61, 138.58, 131.44, 128.11, 127.87, 127.74, 127.67, 123.95, 118.91, 115.14, 98.42, 51.62, 34.94, 32.08, 29.97, 29.02.HRMS (ESI): m/z $[M+H]^+$. Calcd for $C_{24}H_{27}N_6O_4$: 463.2094; found 463.2081.

N-methyl-N-(1-(2-((1-methyl-1H-pyrazol-5-yl) amino) benzoyl) piperidin-4-yl)-4-methoxy-benzamide (9b)

Yellow solid, yield: 72%, m.p. 162~163 °C.^{1}H-NMR (300 MHz, $CDCl_3$) δ (ppm): 7.47 (d, J = 1.80 Hz, 1H, ArH), 7.38 (d, J = 8.70 Hz, 2H, ArH), 7.29(s, 1H, NH), 7.24-7.21 (m, 2H, ArH), 6.94 (d, J = 8.70 Hz, 2H, ArH), 6.87 (t, J = 7.40 Hz, 1H, ArH), 6.81 (d, J = 8.20 Hz, 1H, ArH), 6.05 (d, J = 1.70 Hz, 1H, ArH), 4.76-4.32 (m, 3H, NCH_3CH, $CON(CH_2)_2$), 3.86 (s,

3H, OCH_3), 3.73 (s, 3H, CH_3), 3.16-2.96 (m, 2H, $CON(CH_2)_2$), 2.91 (s, 3H, CH_3), 1.93-1.74(m, 4H, NCH3CH$(CH_2)_2$). ^{13}C-NMR (75 MHz, $CDCl_3$) δ (ppm): 171.63, 169.97, 160.73, 144.08, 139.87, 138.59, 131.30, 128.94, 128.68, 128.11, 119.88, 118.90, 115.04, 113.78, 98.49, 55.33, 50.97, 34.95, 29.74, 29.43, 27.61.HRMS (ESI): m/z $[M+H]^+$. Calcd for $C_{25}H_{30}N_5O_3$: 448.2349; found 448.2338.

N-methyl-N-(1-(2-((1-methyl-1H-pyrazol-5-yl) amino) benzoyl) piperidin-4-yl)-4-fluoro-benzamide (9c)

Gray solid, yield: 58%, m.p. 87~88 °C.^{1}H-NMR (300 MHz, $CDCl_3$) δ (ppm): 7.47-7.42 (m, 3H, ArH), 7.28-7.20 (m, 3H, ArH, NH), 7.15-7.09 (m, 2H, ArH), 6.89-6.80 (m, 2H, ArH), 6.04 (s, 1H, ArH), 5.02-4.60 (m, 1H, CH_3NCH), 4.60-4.20 (m, 2H, $CON(CH_2)_2$), 3.72 (s, 3H, CH_3), 3.23-2.97 (m, 2H, $CON(CH_2)_2$), 2.89 (s, 3H, CH_3), 1.92-1.80 (m, 4H, $CH(CH_2)_2$).^{13}C-NMR (75 MHz, $CDCl_3$) δ (ppm): 170.75, 170.01, 163.34 (d, J = 250.20 Hz), 144.12, 139.86, 138.57, 132.59, 131.35, 129.00, 128.11, 119.73, 118.91, 115.63 (d, J = 21.70 Hz), 115.09, 98.46, 45.05, 34.94, 29.66, 29.36, 28.83.HRMS (ESI): m/z $[M+H]^+$. Calcd for $C_{24}H_{27}FN_5O_2$: 436.2149; found 436.2141.

N-methyl-N-(1-(2-((1-methyl-1H-pyrazol-5-yl) amino) benzoyl) piperidin-4-yl)-4- cyano-benzamide (9d)

Yellow solid, yield: 55%, m.p. 204~205 °C.^{1}H-NMR (300 MHz, $CDCl_3$) δ (ppm): 7.74 (d, J = 7.50 Hz, 2H, ArH), 7.61-7.35 (m, 3H, ArH),

7.29-7.20 (m, 3H, ArH, NH), 6.9-6.81 (m, 2H, ArH), 6.04 (s, 1H, ArH), 4.92-4.72 (m, 1H, CH_3NCH), 4.69-4.24 (m, 2H, $CON(CH_2)_2$), 3.72 (s, 3H, CH_3), 3.22-2.97 (m, 2H, $CON(CH_2)_2$), 2.83 (s, 3H, CH_3), 1.98-1.81 (m, 4H, $CH(CH_2)_2$).^{13}C-NMR (75 MHz, $CDCl_3$) δ (ppm): 170.04, 169.58, 144.17, 140.84, 139.84, 138.58, 132.49, 131.42, 128.11, 127.57, 127.48, 118.91, 117.94, 115.13, 113.58, 98.43, 51.55, 34.94, 32.14, 29.04, 27.93.HRMS (ESI): m/z $[M+H]^+$. Calcd for $C_{25}H_{27}N_6O_2$: 443.2195; found 443.2185.

N-methyl-N-(1-(2-((1-methyl-1H-pyrazol-5-yl) amino) benzoyl) piperidin-4-yl)-4- trifluoromethyl-benzamide (9e)

Yellow solid, yield: 63%, m.p. 187~188 °C.^{1}H-NMR (300 MHz, $CDCl_3$) δ (ppm): 7.70 (d, J = 7.40 Hz, 2H, ArH), 7.60-7.38 (m, 3H, ArH), 7.35-7.20 (m, 3H, ArH, NH), 6.89-6.80 (m, 2H, ArH), 6.04 (s, 1H, ArH), 5.04-4.74 (m, 1H, CH_3NCH), 4.72-4.26 (m, 2H, $CON(CH_2)_2$), 3.72 (s, 3H, CH_3), 3.30-3.02 (m, 2H, $CON(CH_2)_2$), 2.85 (s, 3H, CH_3), 2.06-1.82 (m, 4H, $CH(CH_2)_2$). ^{13}C-NMR (75 MHz, $CDCl_3$) δ (ppm): 172.68, 170.02, 144.14, 140.08, 139.85, 138.57, 131.39, 128.10, 127.19, 126.98, 125.69, 121.35 (q, J = 271.20 Hz), 119.55, 118.90, 115.10, 98.45, 51.34, 34.93, 32.05, 30.03, 29.14.HRMS (ESI): m/z $[M+H]^+$. Calcd for $C_{25}H_{27}F_3N_5O_2$: 486.2117; found 486.2101.

N-methyl-N-(1-(2-((1-methyl-1H-pyrazol-5-yl) amino) benzoyl) piperidin-4-yl)-4-acetyl-benzamide (9f)

Gray solid, yield: 51%, m.p. 177~178°C.^{1}H-NMR (300 MHz, $CDCl_3$) δ (ppm): 8.02 (d, J = 8.00 Hz, 2H, ArH), 7.50-7.40 (m, 3H, ArH), 7.40-7.13 (m, 3H, ArH, NH), 6.89-6.80 (m, 2H, ArH), 6.04 (s, 1H, ArH), 5.03-4.72 (m, 1H, CH_3NCH), 4.69-4.28 (m, 2H, $CON(CH_2)_2$), 3.72 (s, 3H, CH_3), 3.30-3.02 (m, 2H, $CON(CH_2)_2$), 2.84 (s, 3H, CH_3), 2.64 (s, 3H, $COCH_3$), 2.03-1.70 (m, 4H, $CH(CH_2)_2$).^{13}C-NMR (75 MHz, $CDCl_3$) δ (ppm): 172.63, 170.56, 170.01, 144.15, 140.92, 139.85, 138.58, 137.82, 131.38, 128.58, 128.10, 127.00, 126.77, 118.90, 115.10, 98.48, 51.36, 34.94, 32.04, 29.67, 29.19, 26.62.HRMS (ESI): m/z $[M+H]^+$. Calcd for $C_{26}H_{30}N_5O_3$: 460.2349; found 460.2338.

_N_-methyl-_N_-(1-(2-((1-methyl-1_H_-pyrazol-5-yl) amino) benzoyl) piperidin-4-yl)-4-methylsulfonyl-benzamide (9g)

Green solid, yield: 73%, m.p. 107~108 °C.^{1}H-NMR (300 MHz, $CDCl_3$) δ (ppm): 8.03 (d, J = 7.70 Hz, 2H, ArH), 7.59 (d, J = 7.80 Hz, 2H, ArH), 7.47 (s, 1H, NH), 7.32-7.23 (m, 3H, ArH), 6.89-6.80 (m, 2H, ArH), 6.04 (s, 1H, ArH), 4.99-4.81 (m, 1H, CH_3NCH), 4.68-4.23 (m, 2H, $CON(CH_2)_2$), 3.72 (s, 3H, SO_2CH_3), 3.23-2.95 (m, 5H, $CONCH_3$, $CON(CH_2)_2$), 2.83 (s, 3H, CH_3), 2.06-1.62 (m, 4H, $CH(CH_2)_2$).^{13}C-NMR (125 MHz, $CDCl_3$) δ (ppm): 170.03, 169.66, 144.11, 141.92, 141.59, 139.90, 138.53, 131.43, 128.13, 128.01, 127.88, 127.76, 118.96, 115.16, 98.40, 51.53, 44.39, 34.94, 32.21, 29.67, 29.02.HRMS (ESI): m/z $[M+H]^+$. Calcd for $C_{25}H_{30}N_5O_4S$: 496.2019; found 496.2004.

N-methyl-N-(1-(2-(phenylamino) nicotinoyl) piperidin-4-yl)-2-trifluoromethyl-4-fluoro-benzamide (19)

White solid, yield: 59%, m.p. 194~195 °C. Major rotamer: ^{1}H-NMR (300 MHz, $CDCl_3$) δ (ppm): 8.26-8.24 (m, 2H, ArH), 7.55-7.50 (m, 2H, ArH), 7.45-7.37 (m, 2H, ArH), 7.30-7.23 (m, 4H, ArH, NH), 7.00-6.95 (m, 1H, ArH), 6.76-6.69 (m, 1H, ArH), 4.93-4.82 (m, 1H, CH_3NCH), 4.68-4.20 (m, 2H, $CON(CH_2)_2$), 3.11-2.85 (m, 2H, $CON(CH_2)_2$), 2.60 (s, 3H, CH_3), 1.86-1.62 (m, 4H, $NCH(CH_2)_2$).Minor rotamer: ^{1}H-NMR (300 MHz, $CDCl_3$) δ (ppm): 8.26-8.24 (m, 2H, ArH), 7.55-7.50 (m, 2H, ArH), 7.45-7.37 (m, 2H, ArH), 7.30-7.23 (m, 4H, ArH, NH), 7.00-6.95 (m, 1H, ArH), 6.76-6.69 (m, 1H, ArH), 4.68-4.20 (m, 2H, $CON(CH_2)_2$), 3.51-3.29 (m, 1H, CH_3NCH), 2.95 (s, 3H, CH_3), 2.80-2.65 (m, 2H, $CON(CH_2)_2$), 1.86-1.62 (m, 4H, $NCH(CH_2)_2$).Major rotamer: ^{13}C-NMR (75 MHz, $CDCl_3$) δ (ppm): 168.48, 167.53, 161.65 (d, J = 251.20 Hz), 153.40, 149.08, 139.41, 135.97, 128.91, 128.80, 128.49, 128.37, 124.08, 121.90, 119.34, 119.23, 119.03 (d, J = 21.10 Hz), 113.95 (ddd, J = 24.40, 9.30, 4.70 Hz), 113.05, 50.40, 31.08, 28.56, 27.84.Minor rotamer: ^{13}C-NMR (75 MHz, $CDCl_3$) δ (ppm): 168.48, 167.53, 161.65 (d, J = 251.20 Hz), 153.40, 149.28, 139.41, 136.12, 128.91, 128.80, 128.49, 128.37, 124.08, 122.00, 119.34, 119.23, 119.03 (d, J = 21.10 Hz), 113.95 (ddd, J = 24.40, 9.30, 4.70 Hz), 112.99, 56.02, 29.32, 28.89, 27.01.HRMS (ESI): m/z $[M+H]^+$. Calcd for $C_{26}H_{25}F_4N_4O_2$: 501.1914; found 501.1903.

(4-(4-Fluoro-2-(trifluoromethyl) benzoyl) piperazin-1-yl) (2-(phenylamino) phenyl) methanone (16b)

Yellow solid, yield: 71%, m.p. 90~91 °C.^{1}H-NMR (300 MHz, $CDCl_3$) δ (ppm): 7.47-7.37 (m, 2H, ArH), 7.35-7.24 (m, 5H, ArH), 7.18 (dd, J = 7.60, 1.40 Hz, 1H, ArH), 7.14-7.06 (m, 2H, ArH), 7.00 (t, J = 7.30 Hz, 1H, ArH), 6.90 (t, J = 7.40 Hz, 1H, ArH), 3.98-3.91 (m, 1H, piperazine-H), 3.88-3.76 (m, 1H, piperazine-H), 3.74-3.60 (m, 3H, piperazine-H), 3.58-3.48 (m, 1H, piperazine-H), 3.25-3.14 (m, 2H, piperazine-H). ^{13}C-NMR (75 MHz, $CDCl_3$) δ (ppm): 169.71, 166.15, 161.85 (d, J = 252.10 Hz), 142.13, 141.43, 130.45, 129.10, 128.99, 128.96, 128.93, 127.57, 124.04, 121.82, 121.39, 119.26, 119.04 (d, J = 21.70 Hz), 118.55, 116.90, 114.37-113.79 (m), 46.61, 41.47.HRMS (ESI): m/z $[M+H]^+$. Calcd for $C_{25}H_{22}F_4N_3O_2$: 472.1648; found 472.1636.

General procedure for the synthesis of 12a-12i

A mixture of **10** (500.00 mg, 0.90 mmol) **11a-11i** (0.90 mmol) $Pd(OAc)_2$ (0.09 mmol) BINAP (0.18 mmol) was dissolved in 10 mLPhMe. The mixture was stirred at 100 °C under N_2 for 12h. After the reaction was completed, solvent was evaporated under reduced pressure and the residue was purification by column chromatography with dichloromethane/ methanol as eluent on silica gel to give the compounds **12a-12i**.

N-methyl-N-(1-(2-(phenylamino) benzoyl)

piperidin-4-yl)-2-trifluoromethyl-4-fluoro-benzamide (12a)

Light yellow solid, yield: 67%, m.p. 164~165 ^{o}C. Major rotamer: ^{1}H-NMR (300 MHz, $CDCl_3$) δ (ppm): 7.45-7.38 (m, 2H, ArH), 7.30-7.20 (m, 6H, ArH), 7.14-7.03 (m, 2H, ArH), 6.96-6.87 (m, 2H, ArH), 4.88-4.78 (m, 1H, CH_3NCH), 4.67-4.00 (m, 2H, $CON(CH_2)_2$), 3.16-2.91 (m, 2H, $CON(CH_2)_2$), 2.47 (s, 3H, CH_3), 1.76-1.58 (m, 4H, $NCH(CH_2)_2$).Minor rotamer: ^{1}H-NMR (300 MHz, $CDCl_3$) δ (ppm): 7.45-7.38 (m, 2H, ArH), 7.30-7.20 (m, 6H, ArH), 7.14-7.03 (m, 2H, ArH), 6.96-6.87 (m, 2H, ArH), 4.67-4.00 (brs, 2H, $CON(CH_2)_2$), 3.4.-3.30 (m, 1H, CH_3NCH), 2.83 (s, 3H, CH_3), 2.72-2.56 (m, 2H, $CON(CH_2)_2$), 1.76-1.58 (m, 4H, $NCH(CH_2)_2$).Major rotamer: ^{13}C-NMR (75 MHz, $CDCl_3$) δ (ppm): 169.35, 167.44, 161.60(d, J = 250.10 Hz), 142.01, 141.26, 141.22, 129.94, 128.95, 128.88, 128.79, 128.47, 128.36, 127.31, 123.64, 120.78, 119.68, 118.97 (d, J = 21.30 Hz), 117.66, 113.89 (dq, J = 9.40, 4.20 Hz), 50.35, 30.78, 28.45, 27.69.Minor rotamer: ^{13}C-NMR (75 MHz, $CDCl_3$) δ (ppm): 169.33, 167.44, 161.60(d, J = 250.10 Hz), 142.01, 141.26, 141.22, 130.03, 128.95, 128.88, 128.79, 128.47, 128.36, 127.15, 123.64, 120.97, 119.68, 118.97 (d, J = 21.30 Hz), 117.66, 113.89 (dq, J = 9.40, 4.20 Hz), 56.08, 29.18, 28.75, 26.81. HRMS (ESI): m/z $[M+H]^+$. Calcd for $C_{27}H_{26}F_4N_3O_2$: 500.1961; found 500.1949.

N-methyl-N-(1-(2-((4- cyano) phenylamino) benzoyl) piperidin-4-yl)-2-trifluoro methyl-4-fluoro-benzamide (12b)

White solid, yield: 63%, m.p. 226~227 °C. Major rotamer: ^{1}H-NMR (300 MHz, $CDCl_3$) δ (ppm): 7.53 (s, 1H, ArH), 7.48-7.45 (m, 3H, ArH), 7.41-7.34 (m, 2H, ArH), 7.29-7.27 (m, 2H, ArH), 7.09 (t, J = 6.00 Hz, 1H, ArH), 7.04-7.01 (m, 2H, ArH), 4.84-4.75 (m, 1H, CH_3NCH), 4.68-3.70 (m, 2H, $CON(CH_2)_2$), 3.24-2.90 (m, 2H, $CON(CH_2)_2$), 2.46 (s, 3H, CH3), 1.76-1.69 (m, 2H, $NCH(CH_2)_2$), 1.69-1.58 (m, 2H, $NCH(CH_2)_2$).Minor rotamer: ^{1}H-NMR (300 MHz, $CDCl_3$) δ (ppm): 7.53 (s, 1H, ArH), 7.48-7.45 (m, 3H, ArH), 7.41-7.34 (m, 2H, ArH), 7.29-7.27 (m, 2H, ArH), 7.09 (t, J = 6.00 Hz, 1H, ArH), 7.04-7.01 (m, 2H, ArH), 4.68-3.70 (m, 2H, $CON(CH_2)_2$), 3.42-3.27 (m, 1H, CH_3NCH), 2.85 (s, 3H. CH3), 2.72-2.57 (m, 2H, $CON(CH_2)_2$), 1.76-1.69 (m, 2H, $NCH(CH_2)_2$), 1.69-1.58 (m, 2H, $NCH(CH_2)_2$).Major rotamer: ^{13}C-NMR (75 MHz, $CDCl_3$) δ (ppm): 169.05, 167.96, 162.14 (d, J = 251.40 Hz), 147.27, 138.81, 133.73, 131.63, 131.31, 130.56, 129.31 (d, J = 8.00 Hz), 128.50 (q, J = 7.50 Hz), 128.04, 124.9 (q, J = 281.20 Hz), 122.8, 121.05, 119.52 (d, J = 21.20 Hz), 119.51, 115.67, 114.43 (d, J = 22.50 Hz), 102.13, 50.82, 31.27, 28.88, 28.23.Minor rotamer: ^{13}C-NMR (75 MHz, $CDCl_3$) δ (ppm): 169.05, 167.53, 162.21 (d, J = 250.00 Hz), 146.95, 139.02, 133.73, 131.63, 131.31, 130.70, 129.31 (d, J = 8.00 Hz), 128.50 (q, J = 7.50 Hz), 127.96, 124.9 (q, J = 281.20 Hz), 122.63, 120.64, 119.52 (d, J = 21.20 Hz), 119.51, 115.86, 114.43 (d, J = 22.50 Hz), 102.45, 56.42, 28.88, 28.23, 27.26.HRMS (ESI): m/z $[M+H]^+$. Calcd for

$C_{28}H_{25}F_4N_4O_2$: 525.1914 found 525.1898.

N-methyl-N-(1-(2-((2-cyanophenyl) amino) benzoyl) piperidin-4-yl)-2-trifluoromethyl-4-fluoro-benzamide (12c)

White solid, yield: 51%, m.p. 187~188 °C. Major rotamer: ^{1}H-NMR (300 MHz, $CDCl_3$) δ (ppm): 7.54-7.49 (m, 1H, ArH), 7.45-7.35 (m, 4H, ArH), 7.33-7.27 (m, 4H, ArH), 7.13-7.08 (m, 1H, ArH), 6.97-6.89 (m, 1H, ArH), 4.88-4.78 (m, 1H, CH_3NCH), 4.60-3.46 (m, 2H, $CON(CH_2)_2$), 3.25-2.95 (m, 2H, $CON(CH_2)_2$), 2.55 (s, 3H, CH_3), 1.90-1.57 (m, 4H, $NCH(CH_2)_2$). Minor rotamer: ^{1}H-NMR (300 MHz, $CDCl_3$) δ (ppm): 7.54-7.49 (m, 1H, ArH), 7.45-7.35 (m, 4H, ArH), 7.33-7.27 (m, 4H, ArH), 7.13-7.08 (m, 1H, ArH), 6.97-6.89 (m, 1H, ArH), 4.60-3.46 (m, 2H, $CON(CH_2)_2$), 3.40-3.28 (m, 1H, CH_3NCH), 2.89 (s, 3H, CH_3), 2.70-2.64 (m, 2H, $CON(CH_2)_2$), 1.90-1.57 (m, 4H, $NCH(CH_2)_2$). Major rotamer: ^{13}C-NMR (75 MHz, $CDCl_3$) δ (ppm): 168.25, 167.45, 161.59 (d, J = 251.10 Hz), 145.71, 138.20, 133.40, 132.75, 131.29, 129.96, 128.94, 128.83, 128.48, 128.38, 127.70, 125.32 (q, J = 183.70 Hz), 122.50, 120.31, 120.04, 119.84, 119.00 (d, J = 21.50 Hz), 116.63, 113.87 (dq, J = 14.70, 5.00 Hz), 50.35, 30.93, 28.67, 27.76.Minor rotamer: ^{13}C-NMR (75 MHz, $CDCl_3$) δ (ppm): 168.25, 167.45, 161.59 (d, J = 251.10 Hz), 145.71, 138.20, 133.47, 132.83, 131.29, 130.06, 128.94, 128.83, 128.48, 128.38, 127.50, 125.32 (q, J = 183.70 Hz), 122.42, 120.31, 120.04, 119.84, 119.00 (d, J = 21.50 Hz), 116.63, 113.87 (dq, J = 14.70, 5.00 Hz),

56.04, 28.67, 27.76, 26.86.HRMS (ESI): m/z $[M+H]^+$. Calcd for $C_{28}H_{25}F_4N_4O_2$: 525.1914; found 525.1899.

N-methyl-N-(1-(2-((4-methoxyphenyl) amino) benzoyl) piperidin-4-yl)-2-tri-fluoromethyl-4-fluoro-benzamide (12d)

White solid, yield: 61%, m.p. 165~166 °C. Major rotamer: ^{1}H-NMR (300 MHz, $CDCl_3$) δ (ppm): 7.45-7.39 (m, 1H, ArH), 7.31 (d, J = 6.50 Hz, 2H, ArH), 7.25-7.00(m, 5H, ArH), 6.85 (d, J = 8.90 Hz, 2H, ArH), 6.82-6.74 (m, 1H, ArH), 4.91-4.80 (m, 1H, CH_3NCH), 4.72-4.20 (m, 2H, $CON(CH_2)_2$), 3.78 (s, 3H, OCH_3), 3.20-2.96 (m, 2H, $CON(CH_2)_2$), 2.57 (s, 3H, CH_3), 1.81-1.59 (m, 4H, $NCH(CH_2)_2$). Minor rotamer: ^{1}H-NMR (300 MHz, $CDCl_3$) δ (ppm): 7.45-7.39 (m, 1H, ArH), 7.31 (d, J = 6.50 Hz, 2H, ArH), 7.25-7.00(m, 5H, ArH), 6.85 (d, J = 8.90 Hz, 2H, ArH), 6.82-6.74 (m, 1H, ArH), 4.72-4.20 (m, 2H, $CON(CH_2)_2$), 3.78 (s, 3H, OCH_3), 3.41-3.30 (m, 1H, CH_3NCH), 2.92 (s, 3H, CH_3), 2.80-2.62 (m, 2H, $CON(CH_2)_2$), 1.81-1.59 (m, 4H, $NCH(CH_2)_2$). Major rotamer: ^{13}C-NMR (125 MHz, $CDCl_3$) δ (ppm): 170.18, 167.94, 162.12 (d, J = 250.00 Hz), 155.47, 144.10, 135.03, 131.83, 130.60, 129.40, 129.34, 127.89, 122.76 (q, J = 270.00 Hz), 122.48, 121.74, 119.46 (d, J = 21.60 Hz), 118.51, 115.73, 114.74, 114.40 (d, J = 24.80 Hz), 55.56, 51.00, 31.42, 29.05, 28.39. Minor rotamer: ^{13}C-NMR (125 MHz, $CDCl_3$) δ (ppm): 170.25, 167.58, 162.18 (d, J = 249.00 Hz), 155.57, 144.13, 134.88, 131.91, 130.69, 129.40, 129.34, 127.73, 122.76 (q, J = 270.00

Hz), 122.48, 121.50, 119.46 (d, J = 21.60 Hz), 118.51(s), 115.73, 114.74, 114.40 (d, J = 24.80 Hz), 56.66, 55.56, 29.84, 29.39, 27.39.HRMS (ESI): m/z $[M+H]^+$. Calcd for $C_{28}H_{28}F_4N_3O_3$: 530.2067; found 530.2056.

N-methyl-N-(1-(2-((2-methoxyphenyl) amino) benzoyl) piperidin-4-yl)-2-triflu-oromethyl-4-fluoro-benzamide (12e)

White solid, yield: 58%, m.p. 219~220 °C. Major rotamer: ^{1}H-NMR (300 MHz, $CDCl_3$) δ (ppm): 7.45-7.35 (m, 2H, ArH), 7.29-7.25 (m, 4H, ArH), 7.17-7.00 (m, 1H, ArH), 7.00-6.91 (m, 1H, ArH), 6.88-6.84 (m, 3H, ArH), 5.10-4.10 (m, 3H, CH_3NCH, $CON(CH_2)_2$), 3.86 (s, 3H, OCH_3), 3.16-2.90 (m, 2H, $CON(CH_2)_2$), 2.44 (s, 3H, CH_3), 1.85-1.47 (m, 4H, $NCH(CH_2)_2$).Minor rotamer: ^{1}H-NMR (300 MHz, $CDCl_3$) δ (ppm): 7.45-7.35 (m, 2H, ArH), 7.29-7.25 (m, 4H, ArH), 7.17-7.00 (m, 1H, ArH), 7.00-6.91 (m, 1H, ArH), 6.88-6.84 (m, 3H, ArH), 5.08-4.09 (m, 2H, $CON(CH_2)_2$), 3.86 (s, 3H, OCH_3), 3.38-3.23 (m, 1H, CH_3NCH), 2.77 (s, 3H, CH_3), 2.69-2.61 (m, 2H, $CON(CH_2)_2$), 1.85-1.47 (m, 4H, $NCH(CH_2)_2$).Major rotamer: ^{13}C-NMR (75 MHz, $CDCl_3$) δ (ppm): 169.07, 167.40, 161.58 (d, J = 250.80 Hz), 148.41, 140.33, 131.75, 129.70, 128.91, 128.80, 128.35, 127.28, 127.16, 120.24, 120.08, 120.10, 120.04, 118.98 (d, J = 21.10 Hz), 118.09, 114.90, 113.87 (ddd, J = 13.80, 8.80, 4.10 Hz), 110.24, 55.21, 50.34, 30.66, 28.36, 27.59.Minor rotamer: ^{13}C-NMR (75 MHz, $CDCl_3$) δ (ppm): 169.07, 167.40, 161.58 (d, J = 250.80 Hz), 148.41, 140.33, 131.75, 129.77, 128.91, 128.80, 128.35,

127.16, 127.12, 120.24, 120.08, 120.10, 120.04, 118.98 (d, J = 21.10 Hz), 118.09, 114.90, 113.87 (ddd, J = 13.80, 8.80, 4.10 Hz), 110.32, 56.08, 55.21, 29.09, 28.63, 26.65.HRMS (ESI): m/z $[M+H]^+$. Calcd for $C_{28}H_{28}F_4N_3O_3$: 530.2067; found 530.2058.

N-methyl-N-(1-(2-(pyridin-4-ylamino) benzoyl) piperidin-4-yl)-2-trifluoromethyl-4-fluoro-benzamide (12f)

Yellow solid, yield: 44%, m.p. 136~137 ^oC. Major rotamer: ^1H-NMR (300 MHz, $CDCl_3$) δ (ppm): 8.40-8.19 (m, 2H, ArH), 7.49-7.29 (m, 7H, ArH, NH), 7.21-7.15 (m, 1H, ArH), 6.93-6.78 (m, 2H, ArH), 5.07-4.48 (m, 2H, CH_3NCH, $CON(CH_2)_2$), 4.19-3.68 (m, 1H, $CON(CH_2)_2$), 3.25-2.91 (m, 2H, $CON(CH_2)_2$), 2.41 (s, 3H, CH_3), 1.92-1.43 (m, 4H, $NCH(CH_2)_2$). Minor rotamer: ^1H-NMR (300 MHz, $CDCl_3$) δ (ppm): 8.40-8.19 (m, 2H, ArH), 7.49-7.29 (m, 7H, ArH, NH), 7.21-7.15 (m, 1H , ArH), 6.93-6.78 (m, 2H, ArH), 5.07-4.48 (m, 1H, $CON(CH_2)_2$), 4.19-3.68 (m, 1H, $CON(CH_2)_2$), 3.42-3.27 (m, 1H, CH_3NCH), 2.85 (s, 3H, CH_3), 2.69-2.58 (m, 2H, $CON(CH_2)_2$), 1.92-1.43 (m, 4H, $NCH(CH_2)_2$). Major rotamer: ^{13}C-NMR (75 MHz, $CDCl_3$) δ (ppm): 168.88, 167.95, 162.13 (d, J = 247.60 Hz), 150.24, 131.63, 130.42, 129.35, 129.24, 128.89 (d, J = 7.90 Hz), 127.85, 123.53, 123.32, 122.33, 122.00, 119.45 (d, J = 21.20 Hz), 114.38 (d, J = 20.20 Hz), 109.94, 109.80, 50.70, 31.17, 28.81, 28.15. Minor rotamer: ^{13}C-NMR (75 MHz, $CDCl_3$) δ (ppm): 168.88, 167.95, 162.13 (d, J = 247.60 Hz), 150.24, 131.63, 130.57, 129.35, 129.24,

128.89 (d, J = 7.90 Hz), 127.85, 123.53, 123.32, 122.33, 122.00, 119.45 (d, J = 21.20 Hz), 114.38 (d, J = 20.20 Hz), 109.94, 109.80, 56.39, 29.58, 29.19, 27.24.HRMS (ESI): m/z $[M+H]^+$. Calcd for $C_{26}H_{25}F_4N_4O_2$: 501.1914; found 501.1900.

N-methyl-N-(1-(2-(pyridin-2-ylamino) benzoyl) piperidin-4-yl)-2-trifluoromethyl-4-fluoro-benzamide (12g)

Light yellow solid, yield: 36%, m.p. 155~156 ^oC. Major rotamer: ^1H-NMR (300 MHz, $CDCl_3$) δ (ppm): 8.30-8.16 (m, 1H, ArH), 8.01 (d, J = 8.3 Hz, 1H, ArH), 7.84-7.66 (m, 2H, ArH), 7.57-7.25 (m, 5H, ArH, NH), 7.17-6.96 (m, 1H, ArH), 6.96-6.67 (m, 2H, ArH), 4.89-4.77 (m, 1H, CH_3NCH), 4.74-3.65 (m, 2H, $CON(CH_2)_2$), 3.21-2.93 (m, 2H, $CON(CH_2)_2$), 2.50 (s, 3H, CH_3), 1.93-1.50 (m, 4H, $NCH(CH_2)_2$). Minor rotamer: ^1H-NMR (300 MHz, $CDCl_3$) δ (ppm): 8.30-8.16 (m, 1H, ArH), 8.01 (d, J = 8.30 Hz, 1H, ArH), 7.84-7.66 (m, 2H, ArH, NH), 7.57-7.25 (m, 5H, ArH), 7.17-6.96 (m, 1H, ArH), 6.96-6.67 (m, 2H, ArH), 4.74-3.65 (m, 2H, $CON(CH_2)_2$), 3.42-3.23 (m, 1H, CH_3NCH), 2.84 (s, 3H, CH_3), 2.69-2.61 (m, 2H, $CON(CH_2)_2$), 1.93-1.50 (m, 4H, $NCH(CH_2)_2$). Major rotamer: ^{13}C-NMR (75 MHz, $CDCl_3$) δ (ppm): 122.64, 169.54, 162.13 (d, J = 258.70 Hz), 155.39, 148.07, 148.01, 138.77, 137.66, 130.43, 129.38, 129.28, 128.96, 128.86, 127.50, 121.82, 121.35, 119.42 (d, J = 20.90 Hz), 115.37, 114.50 (d, J = 4.50 Hz), 109.98, 50.84, 31.26, 28.94, 28.16. Minor rotamer: ^{13}C-NMR (75 MHz, $CDCl_3$) δ

(ppm): 122.64, 169.54, 162.13 (d, J = 258.70 Hz), 155.39, 148.07, 148.01, 138.77, 137.75, 130.52, 129.38, 129.28, 128.96, 128.86, 127.37, 121.82, 121.35, 119.42 (d, J = 20.90 Hz), 115.54, 114.17 (d, J = 4.10 Hz), 109.98, 56.50, 29.16, 28.45, 27.23. HRMS (ESI): m/z $[M+H]^+$. Calcd for $C_{26}H_{25}F_4N_4O_2$: 501.1914; found 501.1903.

N-methyl-N-(1-(2-([1, 1'-biphenyl]-4-ylamino) benzoyl) piperidin-4-yl)-2-triflu-oromethyl-4-fluoro-benzamide (12h)

Yellow solid, yield: 66%, m.p. 112~113 °C. Major rotamer: ^{1}H-NMR (500 MHz, $CDCl_3$) δ (ppm): 7.62-7.49 (m, 5H, ArH), 7.49-7.38 (m, 3H, ArH), 7.38-7.25 (m, 5H, ArH, NH), 7.19-7.16 (m, 3H, ArH), 6.99 (t, J = 7.50 Hz, 1H, ArH), 4.91-4.84 (m, 1H, CH_3NCH), 4.82-3.79 (m, 2H, $CON(CH_2)_2$), 3.30-2.95 (m, 2H, $CON(CH_2)_2$), 2.52 (s, 3H, CH_3), 1.84-1.73 (m, 2H, $NCH(CH_2)_2$), 1.69-1.62 (m, 2H, $NCH(CH_2)_2$).Minor rotamer: ^{1}H-NMR (500 MHz, $CDCl_3$) δ (ppm): 7.62-7.49 (m, 5H, ArH), 7.49-7.38 (m, 3H, ArH), 7.38-7.25 (m, 5H, ArH, NH), 7.19-7.16 (m, 3H, ArH), 6.99 (t, J = 7.50 Hz, 1H, ArH), 4.82-3.79 (m, 2H, $CON(CH_2)_2$), 3.47-3.28 (m, 1H, CH_3NCH), 2.89 (s, 3H, CH_3), 2.73-2.64 (m, 2H, $CON(CH_2)_2$), 1.84-1.73 (m, 2H, $NCH(CH_2)_2$), 1.69-1.62 (m, 2H, $NCH(CH_2)_2$).Major rotamer: ^{13}C-NMR (125MHz, $CDCl_3$) δ (ppm): 169.81, 167.92, 162.09 (d, J = 249.87 Hz), 141.99, 141.62, 140.69, 134.08, 131.77 (dd, J = 4.30, 2.30 Hz), 130.48, 129.32 (d, J = 8.10 Hz), 128.92 (dd, J = 16.10, 7.30 Hz), 128.72, 127.97, 127.88, 126.67, 126.46,

122.99 (q, J = 261.25 Hz), 120.33, 119.43 (d, J = 20.80 Hz), 118.49, 118.28, 118.24, 114.35 (dd, J = 24.80, 4.60 Hz), 50.89, 31.27, 28.94, 28.21.Minor rotamer: ^{13}C-NMR (125MHz, $CDCl_3$) δ (ppm): 169.77, 167.54, 162.21 (d, J = 250.25 Hz), 141.81, 141.66, 140.63, 134.31, 131.77 (dd, J = 4.30, 2.30 Hz), 130.58, 129.32 (d, J = 8.10 Hz), 128.92 (dd, J = 16.10, 7.30 Hz), 128.77, 128.03, 127.71, 126.75, 126.50, 122.99 (q, J = 261.250 Hz), 120.33, 119.43 (d, J = 20.80 Hz), 118.49, 118.28, 118.24, 114.35 (dd, J = 24.80, 4.60 Hz), 56.59, 29.72, 29.31, 27.27.HRMS (ESI): m/z $[M+H]^+$. Calcd for $C_{33}H_{30}F_4N_3O_2$: 576.2274; found 576.2257.

N-methyl-N-(1-(2-((4-carboxylphenyl) amino) benzoyl) piperidin-4-yl)-2-trifluo-romethyl-4-fluoro-benzamide (12i)

White solid, yield: 43%, m.p. 178~179 °C. Major rotamer: ^{1}H-NMR (300 MHz, $CDCl_3$) δ (ppm): 8.16-7.92 (m, 2H, ArH), 7.55-7.51 (m, 2H, ArH), 7.46-7.30 (m, 4H, ArH), 7.22-7.01 (m, 3H, ArH), 4.87-4.79 (m, 1H, CH_3NCH), 4.40-3.54 (m, 2H, $CON(CH_2)_2$), 3.17-2.93 (m, 2H, $CON(CH_2)_2$), 2.41 (s, 3H, CH_3), 1.93-1.41 (m, 4H, $NCH(CH_2)_2$).Minor rotamer: ^{1}H-NMR (300 MHz, $CDCl_3$) δ (ppm): 8.16-7.92 (m, 2H, ArH), 7.55-7.51 (m, 2H, ArH), 7.46-7.30 (m, 4H, ArH), 7.22-7.01 (m, 3H, ArH), 4.40-3.54 (m, 2H, $CON(CH_2)_2$), 3.39-3.32 (m, 1H, CH_3NCH), 3.17-2.93 (m, 2H, $CON(CH_2)_2$), 2.80 (s, 3H, CH_3), 1.93-1.41 (m, 4H, $NCH(CH_2)_2$).Major rotamer: ^{13}C-NMR (75 MHz, $CDCl_3$) δ (ppm):

170.84, 169.34, 167.99, 162.09 (d, J = 250.50 Hz), 156.98, 148.45, 139.09, 132.16, 130.46, 129.36, 129.26, 128.98, 127.81, 124.42 (q, J = 206.30 Hz), 122.78, 121.53, 120.43, 119.46 (d, J = 20.80 Hz), 114.88, 114.37 (d, J = 20.60 Hz), 50.73, 31.16, 28.81, 28.10.Minor rotamer: ^{13}C-NMR (75 MHz, $CDCl_3$) δ (ppm): 170.72, 169.34, 167.99, 162.09 (d, J = 250.50 Hz), 156.98, 148.45, 139.09, 132.16, 130.58, 129.36, 129.26, 128.98, 127.68, 124.42 (q, J = 206.30 Hz), 122.78, 121.32, 120.74, 119.46 (d, J = 20.80 Hz), 114.88, 114.37 (d, J = 20.60 Hz), 56.41, 29.63, 29.15, 27.20.HRMS (ESI): m/z $[M+H]^+$·Calcd for $C_{28}H_{26}F_4N_3O_4$: 544.1859; found 544.1845.

4.2 Biological Assay

4.2.1 Gli-luciferase Reporter Assay

Cells were seeded in 96-wellplates, followed by various treatments as indicated. The luciferaseactivity in the cell lysates was measured using a Dual-LuciferaseReporter Assay System (Promega) according to the manufacturer'sinstructions in a luminometer (Molecular Devices; Sunnyvale, CA). The firefly luciferase values were normalized to Renilla values.

4.2.2 MTT Assay

The human medulloblastoma cell line Daoywas purchased from American Tissue Culture Collection (ATCC, Rockville, MD, USA). The human melanoma cell line A2058 was purchased from Chinese Academy

of Sciences Cell Bankand. Daoy cells were cultured in RPMI-1640 supplemented with 10% Fetal Bovine Serum (FBS, ScienCell), while A2058 cells were cultured in DMEM-H (KeyGENBioTECH) also supplemented with 10% FBS. Cells were seeded into 96-well plates in three re-plates (100 μL/well) with a density of 5×10^3 cells/well. After incubated at 37 °C overnight in a humidified 5% CO_2 incubator, vehicle or the test compounds at different concentrations (100 μL/well) were added to each well. After incubation at 37 °C for 72 h, the cell viability was determined using a MTT assay. The IC_{50} was defined as the concentration of compound required to inhibit cell proliferation by 50%. The data were analysed with GraphPad Prism 6.

4.3 Computational experiments

4.3.1 Molecular docking

The protein co-crystallized with LY2940680, was downloaded from the PDB (PDB code: 4JKV). Protein Preparation Wizard of the Schrödinger Suite was used to prepare protein structure. Small molecules were prepared using LigPrep prior to docking simulation. The Glide implemented in Schrödinger 2013 was used to molecular docking. The standard precision (SP) mode was used for the docking and scoring. All other parameters were kept default. The best pose was output on the basis of Glide score and the protein-ligand interactions.

4.3.2 Molecular Dynamic

Molecular dynamics simulations were performed using Discovery studio 2.5 Standard Dynamics Cascade and the Charmm 27 force field was used to simulate these complexes. The topology files for LY2940680, 12a were generated using PRODRG. 4 ns production run was performed in an NPT ensemble using an isotropic Parrinello−Rahman pressure coupling, Nose-Hover thermostat at 300 K and periodic boundary conditions.

Binding free energy was calculated for these compounds using Prime mmgbsa tool of the Schrödinger Suite. After the MD simulation was finished, 10 snapshots from the equilibrium period of the MD trajectory with one snapshot for every 100 ps were extracted and subject to binding free energy calculation.

Acknowledgement

This work was supported by the Funding of Double First-rate Discipline Innovation Teams(CPU2018GY05).

Conflicts of interest

The authors declare no conflicts of interest.

References:

[1] I. Galperin, L.Dempwolff, W.E. Diederich, M. Lauth, Inhibiting Hedgehog: An Update on Pharmacological Compounds and Targeting

Strategies,J. Med. Chem.,62(2019)8392-8411.

[2] S. Pietrobono, B. Stecca, Targeting the Oncoprotein Smoothened by Small Molecules: Focus on Novel Acylguanidine Derivatives as Potent Smoothened Inhibitors, Cells, 7(2018) 272-302.

[3] J. Briscoe, P.P. Thérond, The mechanisms of Hedgehog signalling and its roles in development and disease, Nat. Rev. Mol. Cell Bio., 14(2013) 416-429.

[4] J. Bariwal, V. Kumar, Y. Dong, R.I. Mahato, Design of Hedgehog pathway inhibitors for cancer treatment, Med. Res. Rev., 39(2019) 1137-1204.

[5] R.L. Carpenter, H. Ray, Safety and Tolerability of Sonic Hedgehog Pathway Inhibitors in Cancer, Drug Saf., 42(2019) 263-279.

[6] FDA approves new treatment for patients with acute myeloid leukemia,FDA News Release November 21, 2018 https://www.fda.gov/news-events/press-announcements/fda-approves-new-treatment-patients-acute-myeloid-leukemia.

[7] M. Xin, X. Ji, L.K. De La Cruz, S. Thareja, B. Wang, Strategies to target the Hedgehog signaling pathway for cancer therapy, Med. Res. Rev., 38(2018) 870-913.

[8] S. Malpel, S. Claret, M. Sanial, A. Brigui, T. Piolot, L. Daviet, S. Martin-Lanneree, A. Plessis, The last 59 amino acids of Smoothened cytoplasmic tail directly bind the protein kinase Fused and negatively

regulate the Hedgehog pathway, Dev. Biol., 303(2007) 121-133.

[9] C. Wang, H. Wu, V. Katritch, G.W. Han, X.P. Huang, W. Liu, F.Y. Siu, B.L. Roth, V. Cherezov, R.C. Stevens, Structure of the human smoothened receptor bound to an antitumour agent, Nature, 497(2013) 338-343.

[10] M.H. Bender, P.A. Hipskind, A.R. Capen, M. Cockman, K.M. Credille, H. Gao, J.A. Bastian, J.M. Clay, K.L. Lobb, D.J. Sall, M. L. Thompson, T. Wilson, G. N. Wishart B. K.R Patel, Abstract 2819: Identification and characterization of a novel smoothened antagonist for the treatment of cancer with deregulated hedgehog signaling, Cancer Res., 71(2011) 2819-2819.

[11] P. Furet, G. Caravatti, V. Guagnano, M. Lang, T. Meyer, J. Schoepfer, Entry into a new class of protein kinase inhibitors by pseudo ring design, Bioorg. Med. Chem. Lett., 18(2008) 897-900.

[12] W. Zhang, D. Zhang, M.A. Stashko, D. DeRyckere, D. Hunter, D. Kireev, M.J. Miley, C. Cummings, M. Lee, J. Norris-Drouin, W.M. Stewart, S. Sather, Y. Zhou, G. Kirkpatrick, M. Machius, W. P. Janzen, H.S. Earp, D.K. Graham, S.V. Frye,Pseudo-cyclization through intramolecular hydrogen bond enables discovery of pyridine substituted pyrimidines as new Mer kinase inhibitors, J. Med. Chem., 56(2013) 9683-9692.

[13] W.G. Harter, H. Albrect, K. Brady, B. Caprathe, J. Dunbar, J.

Gilmore, S. Hays, C.R. Kostlan, B. Lunney, N. Walker, The design and synthesis of sulfonamides as caspase-1 inhibitors, Bioorg.Med. Chem. Lett., 14(2004) 809-812.

[14] P. Furet, G. Bold, F. Hofmann, P. Manley, T. Meyer, K.-H. Altmann, Identification of a new chemical class of potent angiogenesis inhibitors based on conformational considerations and database searching, Bioorg.Med. Chem. Lett., 13(2003) 2967-2971.

[15] S.F. Martin, J.H. Clements, Correlating Structure and Energetics in Protein-Ligand Interactions: Paradigms and Paradoxes, Annu. Rev.Biochem., 82(2013) 267-293.

[16] M.H. Bender, P.A. Hipskind, A.R. Capen, M. Cockman, K.M. Credille, H. Gao, J.A. Bastian, J.M. Clay, K.L. Lobb, D.J. Sall, M. L. Thompson, T. Wilson, G. N. Wishart, B. K. R Patel, Abstract 2819: Identification and characterization of a novel smoothened antagonist for the treatment of cancer with deregulated hedgehog signaling, Cancer Res., 71(2011) 2819-2819.

[17] G. Juin, R. G. de O. Junior, A. Fleury, C. Oudinet, L. Pytowski, J.-B. Bérard, E. Nicolau, V. Thiéry, I. Lanneluc, L. Beaugeard, G. Prunier, J. R. G. D. S. Almeida, L. Picot, Zeaxanthin from Porphridium Purpureum induces apoptosis in human melanoma cells expressing the oncogenic BRAF V600E mutation and sensitizes them to the BRAF inhibitor vemurafenib, Rev. Bras. Farmacogn., 28(2018) 457-467.

Conflicts of interest

The authors declare no conflicts of interest.